

Statistical inference for the two-sample problem under likelihood ratio ordering, with application to the ROC curve estimation

Dingding Hu¹, Meng Yuan¹, Tao Yu² and Pengfei Li¹

¹Department of Statistics and Actuarial Sciences, University of Waterloo, Waterloo, ON, N2L 3G1, Canada

²Department of Statistics and Data Science, National University of Singapore, 117546, Singapore

Abstract: The receiver operating characteristic (ROC) curve is a powerful statistical tool and has been widely applied in medical research. In the ROC curve estimation, a commonly used assumption is that larger the biomarker value, greater severity the disease. In this paper, we mathematically interpret “greater severity of the disease” as “larger probability of being diseased”. This in turn is equivalent to assume the likelihood ratio ordering of the biomarker between the diseased and healthy individuals. With this assumption, we first propose a Bernstein polynomial method to model the distributions of both samples; we then estimate the distributions by the maximum empirical likelihood principle. The ROC curve estimate and the associated summary statistics are obtained subsequently. Theoretically, we establish the asymptotic consistency of our estimators. Via extensive numerical studies, we compare the performance of our method with competitive methods. The application of our method is illustrated by a real-data example.

Keywords: Area under the ROC curve, Bernstein polynomials, Likelihood ratio ordering, ROC curve, Youden index.

1 Introduction

The ROC curve is a powerful statistical tool and has been widely applied in many scientific areas; it evaluates the diagnostic abilities of a binary classifier for varied discrimination thresholds. Consider a medical study, where a biomarker serves as a binary classifier for diagnosing the healthy/diseased status of each patient. The ROC curve plots the “sensitivity” against “one minus the specificity” at all the possible thresholds of the biomarker. Here, sensitivity/specificity refers to the probability of correctly identifying the diseased/healthy individuals. The ROC curve related inferences have been extensively investigated in the literature; we refer to Pepe (2003), Zhou et al. (2011), Qin and Zhang (2003), and Chen et al. (2016) for a comprehensive review of the existing developments.

Practically, for an individual, we may assume that the larger biomarker value indicates greater possibility/severity of the disease; therefore, we can classify individuals as diseased if their corresponding biomarkers exceed a given cutoff point x , and vice versa; see Yin and Tian (2014) for a discussion. Under this assumption, the sensitivity and specificity are $1 - F_1(x)$ and $F_0(x)$, where $F_0(\cdot)$ and $F_1(\cdot)$ denote the cumulative distribution functions (cdfs) of the biomarkers for individuals that are healthy and diseased, respectively. The ROC curve is then given by

$$ROC(s) = 1 - F_1(F_0^{-1}(1 - s)),$$

for $s \in (0, 1)$.

In the literature, there are two common strategies for mathematically accommodating the assumption that larger biomarker associates with the greater severity of the disease. The first interprets it as the biomarker values of diseased individuals are stochastically greater than those of healthy ones; that is $F_1(x) \leq F_0(x)$ for every $x \in \mathbb{R}$ (Wang et al., 2017). The second assumes that larger biomarker value corresponds to larger probability of getting the disease (Yu et al., 2017); with the assumption that “the larger biomarker value indicates greater severity of the disease”, this second strategy is equivalent to interpret “greater severity of the disease” as “larger probability of being diseased”. More specifically, let X and D denote the biomarker and indicator of the membership of an individual: $D = 1$ or 0 respectively indicates that the individual is diseased or healthy. Using Bayes’ formula, we have

$$P(D = 1|X = x) = \frac{P(D = 1)f_1(x)}{P(D = 1)f_1(x) + P(D = 0)f_0(x)}; \quad (1)$$

where $f_1(x)$ and $f_0(x)$ are the probability density functions (pdfs) of the biomarkers in the diseased population and the healthy population, respectively. Hence, the second interpretation equivalently assumes that $f_1(x)/f_0(x)$ is a monotone function of x , which is known as the likelihood ratio ordering (Yu et al., 2017; Dykstra et al., 1995). We observe that with the likelihood ratio ordering, the derivative of $ROC(s)$,

$$\frac{d\{ROC(s)\}}{ds} = \frac{f_0(F_1^{-1}(1-s))}{f_1(F_1^{-1}(1-s))},$$

is nonincreasing, which implies that $ROC(s)$ is concave for $s \in (0, 1)$. We refer to Gneiting and Vogel (2018) for the importance of concavity in the interpretation and modelling of ROC curves. Furthermore, we observe that as an assumption, likelihood ratio ordering is also widely adopted in many important applications of the Neyman–Pearson lemma, such as the Karlin–Rubin theorem. In this paper, we shall incorporate the likelihood ratio ordering assumption to improve the estimation of ROC curve and its summary statistics.

There are three types of estimation methods for the ROC curves: the parametric, the semiparametric (Zhou and Lin, 2008), and the nonparametric methods (Zhou et al., 2011). We observe that many of these estimation methods did not incorporate the likelihood ratio ordering constraint; ignoring this constraint may result in less accurate ROC estimation. As far as we are aware, they are two estimation methods in the literature that have accommodated this constraint: Dykstra et al. (1995) considered the estimation of F_0 and F_1 with a maximum nonparametric likelihood approach; Yu et al. (2017) proposed a smoothed likelihood approach to estimate f_0 and f_1 . The former leads to a non-smooth estimate of $P(D = 1|X = x)$ in (1), and therefore the resulting estimate of the optimal cutoff point that maximizes the Youden index is inefficient. See Section 1 of the supplementary material for more details. The latter relies on a smoothing parameter the optimal choice of which is not easily obtained.

In this paper, we propose a Bernstein polynomial method that accommodates the likelihood ratio ordering assumption, and use the empirical likelihood principle to estimate F_0 , F_1 , ROC curve, and two popular summary statistics: the area under the curve (AUC) and the Youden index (Youden, 1950). With the help of the existing R function `glmnet` (Friedman et al., 2010), we establish an algorithm to implement our proposed method; we integrate our algorithm as an R package BPLR available at “<https://github.com/Dingding-Hu/BPLR-package>”. We have also established the asymptotic consistency of our method. It is noteworthy that the resulting estimate of $P(D = 1|X = x)$ from our method is smooth; through extensive numerical studies, we observe that our ROC curve, Youden index, and the associated optimal cutoff point estimates outperform those from the existing methods in most examples.

The rest of the paper is organized as follows. Section 2 proposes the Bernstein polynomial method with the empirical likelihood principle to establish the estimators for $F_0(\cdot)$ and $F_1(\cdot)$, and subsequently result in the estimators of the ROC curve and its summary statistics. The consistency of the proposed method is also studied. Section 3 presents the simulation results. Section 4 compares our method with existing methods in a real-data example, and Section 5 concludes the paper with some discussion. Technical details are given in the supplementary material.

2 Main results

2.1 Bernstein polynomials approach

Denote by $\{X_1, \dots, X_{n_0}\}$ and $\{Y_1, \dots, Y_{n_1}\}$ the random samples of biomarkers from the healthy and the diseased populations, respectively. The pdf and cdf of X_i 's are f_0 and F_0 ; the pdf and cdf of Y_j 's are f_1 and F_1 . Let $n = n_0 + n_1$ be the total sample size; denote by $t_1 < \dots < t_m$ the distinct values of the combined sample.

We assume that f_0 and f_1 satisfy the likelihood ratio ordering, i.e., $f_1(x)/f_0(x)$ is an increasing function of x . To incorporate this constraint in the estimation procedure, we propose to model $\log\{f_1(x)/f_0(x)\}$ as a linear combination of Bernstein polynomials. The definition of the Bernstein polynomials is given below.

Definition 1. (*Bernstein polynomials*) Let N be a positive integer. For each $0 \leq l \leq N$, the Bernstein polynomials are defined to be

$$B_l(x; N) = \binom{N}{l} x^l (1-x)^{N-l}, \quad l = 0, \dots, N, \quad x \in [0, 1].$$

Bernstein polynomials can serve as a set of base functions in the expansion of a nonparametric component. A nice feature of such an expansion is that it is able to incorporate the shape constraints as some condition(s) of the coefficients of polynomials. For a monotonic nonparametric component, we can expand it to be $\sum_{l=0}^N \beta_l B_l(x; N)$, which is an increasing function of x if

$$\beta_0 \leq \beta_1 \leq \dots \leq \beta_N. \quad (2)$$

We refer to Wang and Ghosh (2012) for more details of incorporating other types of shape constraints in the Bernstein polynomial expansion.

Next, we apply the Bernstein polynomials to our estimation problem. For presentational convenience, in the development below, we assume that N is given and all biomarkers are ranged in $[0, 1]$. Remarks 1 and 2 give the solutions of how to choose N and transform the biomarkers so that they are contained in $[0, 1]$ in practice. Based on the likelihood ratio ordering assumption, $\log\{f_1(x)/f_0(x)\}$ is an increasing function of x . We propose to model it by a linear combination of Bernstein polynomials:

$$\log\{f_1(x)/f_0(x)\} = \sum_{l=0}^N \beta_l B_l(x; N), \quad (3)$$

with $(\beta_0, \dots, \beta_N)$ satisfying (2); and then incorporate the maximum empirical likelihood to estimate $(\beta_0, \dots, \beta_N)$, F_0 , and F_1 . To this end, let

$$a_i = \sum_{j=1}^{n_0} I(X_j = t_i) \quad \text{and} \quad b_i = \sum_{j=1}^{n_1} I(Y_j = t_i).$$

Based on the observed two-sample data, the full likelihood function is given by

$$L = \prod_{i=1}^m \{f_0(t_i)^{a_i} \cdot \{f_1(t_i)\}^{b_i}.$$

For $i = 1, \dots, m$, let

$$p_{i0} = f_0(t_i) \quad \text{and} \quad p_{i1} = f_1(t_i).$$

Then, the empirical likelihood (Owen, 2001) is

$$L = \prod_{i=1}^m p_{i0}^{a_i} \cdot p_{i1}^{b_i}.$$

We assume $n_1/n \rightarrow \lambda \in (0, 1)$ as $n \rightarrow \infty$. For simplicity, hereafter we write $\lambda = n_1/n$ and assume that it is constant, since it does not affect our technical development. We further define

$$\phi_i = (1 - \lambda)f_0(t_i) + \lambda f_1(t_i) = (1 - \lambda)p_{i0} + \lambda p_{i1}.$$

By model (3), we have

$$\begin{aligned} p_{i0} &= \frac{\phi_i}{1 - \lambda + \lambda \exp \left\{ \sum_{l=0}^N \beta_l B_l(t_i; N) \right\}}, \\ p_{i1} &= \frac{\exp \left\{ \sum_{l=0}^N \beta_l B_l(t_i; N) \right\} \phi_i}{1 - \lambda + \lambda \exp \left\{ \sum_{l=0}^N \beta_l B_l(t_i; N) \right\}}. \end{aligned}$$

That is, p_{i0} 's and p_{i1} 's are determined by ϕ_i 's and $(\beta_0, \dots, \beta_N)$.

With the above reparameterization, the empirical likelihood function of $(\phi_1, \dots, \phi_m, \beta_0, \dots, \beta_N)$ is then given as

$$L = \prod_{i=1}^m p_{i0}^{a_i} p_{i1}^{b_i} = (\lambda)^{-n_1} (1 - \lambda)^{-n_0} \cdot L_1(\phi_1, \dots, \phi_m) \cdot L_2(\beta_0, \dots, \beta_N),$$

where

$$L_1(\phi_1, \dots, \phi_m) = \prod_{i=1}^m \phi_i^{a_i + b_i} \quad \text{and} \quad L_2(\beta_0, \dots, \beta_N) = \prod_{i=1}^m \left[\{\theta(t_i)\}^{b_i} \{1 - \theta(t_i)\}^{a_i} \right]$$

with

$$\theta(x) = \frac{\lambda \exp \left\{ \sum_{l=0}^N \beta_l B_l(x; N) \right\}}{1 - \lambda + \lambda \exp \left\{ \sum_{l=0}^N \beta_l B_l(x; N) \right\}}.$$

Note that feasible ϕ_i 's satisfy

$$\phi_i \geq 0, \quad \sum_{i=1}^m \phi_i = 1 \tag{4}$$

and

$$\sum_{i=1}^m \phi_i \theta(t_i) = \lambda \tag{5}$$

to ensure that both F_0 and F_1 are cdfs. The maximum empirical likelihood estimator (MELE) of $(\phi_1, \dots, \phi_m, \beta_0, \dots, \beta_N)$ is then defined to be

$$(\hat{\phi}_1, \dots, \hat{\phi}_m, \hat{\beta}_0, \dots, \hat{\beta}_N) = \arg \max_{\phi_1, \dots, \phi_m, \beta_0, \dots, \beta_N} L$$

subject to constraints (4), (5), and the inequality constraints in (2).

To solve the optimization problem above, we consider the following reparameterization of β_l 's:

$$\beta_0 = \alpha_0, \quad \beta_1 = \alpha_0 + \alpha_1, \dots, \beta_N = \sum_{l=0}^N \alpha_l.$$

Then (2) is equivalent to

$$\alpha_1 \geq 0, \dots, \alpha_N \geq 0.$$

The above reparameterization implies that

$$\sum_{l=0}^N \beta_l B_l(x; N) = \sum_{l=0}^N \alpha_l B_l^*(x; N),$$

where $B_l^*(x; N) = \sum_{k=l}^N B_k(x; N)$ for $l = 1, \dots, N$ and $B_0^*(x; N) = 1$.

With a slight abuse of notation, we write

$$L_2(\alpha_0, \dots, \alpha_N) = \prod_{i=1}^m \left[\{\theta(t_i)\}^{b_i} \{1 - \theta(t_i)\}^{a_i} \right]$$

with

$$\theta(x) = \frac{\lambda \exp \left\{ \alpha_0 + \sum_{l=1}^N \alpha_l B_l^*(x; N) \right\}}{1 - \lambda + \lambda \exp \left\{ \alpha_0 + \sum_{l=1}^N \alpha_l B_l^*(x; N) \right\}}.$$

The following proposition summarizes the results for calculating the MELEs of ϕ_i 's and $(\alpha_0, \alpha_1, \dots, \alpha_N)$. The proof is given in the supplementary material.

Proposition 1. *Let*

$$(\hat{\phi}_1, \dots, \hat{\phi}_m) = \arg \max_{\phi_1, \dots, \phi_m} L_1(\phi_1, \dots, \phi_m) \text{ subject to (4)}$$

and

$$(\hat{\alpha}_0, \dots, \hat{\alpha}_N) = \arg \max_{\alpha_0, \dots, \alpha_N} L_2(\alpha_0, \dots, \alpha_N)$$

subject to $\alpha_l \geq 0$ for $l = 1, \dots, N$. Then

(a) $\hat{\phi}_i = (a_i + b_i)/n$ for $i = 1, \dots, m$;

(b) $\sum_{i=1}^m \hat{\phi}_i \hat{\theta}(t_i) = \lambda$, where

$$\hat{\theta}(x) = \frac{\lambda \exp \left\{ \hat{\alpha}_0 + \sum_{l=1}^N \hat{\alpha}_l B_l^*(x; N) \right\}}{1 - \lambda + \lambda \exp \left\{ \hat{\alpha}_0 + \sum_{l=1}^N \hat{\alpha}_l B_l^*(x; N) \right\}}. \quad (6)$$

Proposition 1 implies that we can maximize L_1 and L_2 separately to obtain the MELEs of ϕ_i 's and $(\alpha_0, \alpha_1, \dots, \alpha_N)$. The MELEs of ϕ_i 's have the closed form in Proposition 1 (a). Note that $L_2(\alpha_0, \dots, \alpha_N)$ can be viewed as the likelihood for the standard logistic regression with the intercept being $\alpha_0 + \log\{\lambda/(1-\lambda)\}$ and covariates being $B_1^*(x; N), \dots, B_N^*(x; N)$. Then $(\hat{\alpha}_0, \dots, \hat{\alpha}_N)$ can be readily calculated by using the existing R function `glmnet`. Once $\hat{\phi}_i$'s and $(\hat{\alpha}_0, \dots, \hat{\alpha}_N)$ are available, the estimates of p_{i0} 's and p_{i1} 's are given by

$$\begin{aligned} \hat{p}_{i0} &= \frac{\hat{\phi}_i}{1 - \lambda + \lambda \exp \left\{ \hat{\alpha}_0 + \sum_{l=1}^N \hat{\alpha}_l B_l^*(t_i; N) \right\}} \\ \hat{p}_{i1} &= \frac{\exp \left\{ \hat{\alpha}_0 + \sum_{l=1}^N \hat{\alpha}_l B_l^*(t_i; N) \right\} \hat{\phi}_i}{1 - \lambda + \lambda \exp \left\{ \hat{\alpha}_0 + \sum_{l=1}^N \hat{\alpha}_l B_l^*(t_i; N) \right\}}, \end{aligned}$$

which lead to the estimates for $F_0(\cdot)$ and $F_1(\cdot)$:

$$\hat{F}_0(x) = \sum_{i=1}^m \hat{p}_{i0} I(t_i \leq x) \quad \text{and} \quad \hat{F}_1(x) = \sum_{i=1}^m \hat{p}_{i1} I(t_i \leq x). \quad (7)$$

We make some remarks for the proposed method above.

Remark 1. *In the development above, we have assumed that N is known. In practice, we can choose it based on the Bayesian information criterion (BIC). Specifically, since we maximize $L_2(\alpha_0, \dots, \alpha_N)$ to obtain the estimators of $(\alpha_0, \dots, \alpha_N)$, we can use it to establish the BIC criterion. For any N , let*

$$(\tilde{\alpha}_0, \tilde{\alpha}_1, \dots, \tilde{\alpha}_N) = \arg \max_{\alpha_0, \dots, \alpha_N} L_2(\alpha_0, \dots, \alpha_N)$$

and

$$\tilde{\theta}(x) = \frac{\lambda \exp \left\{ \tilde{\alpha}_0 + \sum_{l=1}^N \tilde{\alpha}_l B_l^*(x; N) \right\}}{1 - \lambda + \lambda \exp \left\{ \hat{\alpha}_0 + \sum_{l=1}^N \tilde{\alpha}_l B_l^*(x; N) \right\}}.$$

That is, $\tilde{\theta}(x)$ is the MELE of $\theta(x)$ without the monotonicity assumption. Denote by df_N the number of unknown parameters in $\theta(x)$. We define

$$BIC(N) = -2 \log \left[\prod_{i=1}^m \{ \tilde{\theta}_N(t_i) \}^{b_i} \{ 1 - \tilde{\theta}_N(t_i) \}^{a_i} \right] + (\log n) \cdot df_N.$$

Consequently, N is set to be the minimizer of $BIC(N)$. We use $\tilde{\theta}(x)$ instead of $\hat{\theta}(x)$ to construct the BIC criterion because without the monotonicity assumption, the number of unknown parameters in $\theta(x)$ can be clearly counted.

Remark 2. Practically, a biomarker, x say, may not be in the range $[0, 1]$. We can consider the transformation

$$x^* = \frac{x - t_{(1)}}{t_{(m)} - t_{(1)}},$$

with $t_{(1)}$ and $t_{(m)}$ being the minimum and the maximum values of t_i 's. Clearly $x^* \in [0, 1]$; we can then apply our method to the transformed biomarkers.

Remark 3. We observe that biomarkers may exhibit high variability in practice; applying a log transformation on them may improve the performance. Furthermore, we may include both the original and transformed biomarkers in the model. Specifically, we may consider

$$\log \{ f_1(x)/f_0(x) \} = \alpha_0 + \sum_{l=1}^N \alpha_l B_l^*(x^*; N) + \sum_{l=1}^N \alpha_{N+l} B_l^*(z^*; N), \quad (8)$$

where

$$z^* = \frac{\log x - \log t_{(1)}}{\log t_{(m)} - \log t_{(1)}},$$

and $\alpha_l \geq 0$ for $l = 1, \dots, (2N)$. All our developments above can be similarly applied to (8). This modelling strategy is applied in all the simulation and real data examples.

Remark 4. Our method is established on the likelihood ratio ordering assumption. To check the rationale of this assumption in practice, we can plot (\hat{F}_0, \hat{F}_1) in (7) and $(\tilde{F}_0, \tilde{F}_1)$, where \tilde{F}_0 and \tilde{F}_1 are respectively the empirical cdfs of $\{X_1, \dots, X_{n_0}\}$ and $\{Y_1, \dots, Y_{n_1}\}$. If the plots of \tilde{F}_i are reasonably close to those of \hat{F}_i for $i = 0, 1$, we may regard the likelihood ratio ordering as a reasonable assumption. More rigorously, we can also use the goodness-of-fit test statistics:

$$\Delta_n = \sup_x |\hat{F}_0(x) - \tilde{F}_0(x)|,$$

and the Bootstrap method to test this assumption.

2.2 Estimation of the ROC curve and its summary statistics

With the estimate $\hat{F}_0(x)$ and $\hat{F}_1(x)$, the ROC curve can be estimated by

$$\widehat{ROC}(s) = 1 - \hat{F}_1 \left(\hat{F}_0^{-1}(1-s) \right). \quad (9)$$

In this paper, we further consider two summary statistics based on the ROC curve: AUC and Youden index. The AUC is the total area under the ROC curve, i.e.,

$$AUC = \int_0^1 ROC(s) ds.$$

Note that for a given threshold or cutoff point of the biomarker, it is desirable to have the corresponding value on y -axis (the sensitivity) to be as large as possible. Hence, the larger AUC value indicates that the binary classifier has stronger classification ability. With $\widehat{ROC}(s)$, AUC can be estimated by

$$\widehat{AUC} = \int_0^1 \widehat{ROC}(s) ds. \quad (10)$$

The Youden index (J) is defined as the maximum value of the sensitivity plus the specificity minus 1, i.e.,

$$J = \max_x \{1 - F_1(x) + F_0(x) - 1\} = \max_x \{F_0(x) - F_1(x)\}.$$

One advantage of Youden index is that it results in a criterion to choose the “optimal” cutoff point, which is the “ x ” where Youden index is achieved. Specifically

$$C = \arg \max_x \{F_0(x) - F_1(x)\}. \quad (11)$$

We refer to Yuan et al. (2021) and the references therein for recent developments in the Youden index and the optimal cutoff point estimation. Note that (11) implies $f_0(C) = f_1(C)$, and hence $\theta(C) = \lambda$. Therefore we can solve the equation

$$\hat{\theta}(\hat{C}) = \lambda \quad (12)$$

to obtain \hat{C} and as a consequence,

$$\hat{J} = \hat{F}_0(\hat{C}) - \hat{F}_1(\hat{C}). \quad (13)$$

2.3 Asymptotic properties

In this section, we establish the consistency of our estimators. We need the following notation. Let $G(x) = \lambda F_1(x) + (1 - \lambda)F_0(x)$ and denote

$$\theta_0(x) = \frac{\lambda f_1(x)}{(1 - \lambda)f_0(x) + \lambda f_1(x)}. \quad (14)$$

We first show the L_2 convergence of $\hat{\theta}(\cdot)$ to $\theta_0(\cdot)$, where $\hat{\theta}(\cdot)$ is defined by (6). For presentational continuity, we give the conditions in the Appendix, and relegate the technical details to the supplementary material.

Theorem 1. *Assume Conditions A1–A3 in the Appendix. We have*

$$\int_0^1 \left\{ \hat{\theta}(x) - \theta_0(x) \right\}^2 dG(x) = o_p(1).$$

With Theorem 1, we are able to establish the asymptotic consistency of (\hat{F}_0, \hat{F}_1) in (7), $\widehat{ROC}(s)$ in (9), \widehat{AUC} in (10), \hat{C} in (12), and \hat{J} in (13); the results are given in Theorem 2 below.

Theorem 2. *Assume Conditions A1–A3 in the Appendix. We have*

- (a) $\sup_{x \in [0,1]} \left| \hat{F}_0(x) - F_0(x) \right| = o_p(1)$ and $\sup_{x \in [0,1]} \left| \hat{F}_1(x) - F_1(x) \right| = o_p(1)$,
- (b) $\sup_{s \in [0,1]} \left| \widehat{ROC}(s) - ROC(s) \right| = o_p(1)$,
- (c) $\widehat{AUC} = AUC + o_p(1)$.

Furthermore, if Condition A4 in the Appendix is also satisfied, then

- (d) $\hat{C} = C + o_p(1)$ and $\hat{J} = J + o_p(1)$.

3 Simulation study

3.1 Simulation setup

In this section, with simulation examples, we compare the performance of our proposed method (denoted as “BP”) with existing methods in the estimation of the ROC curves and its summary statistics. We consider the following seven competitive methods:

- the Box-Cox method in Bantis et al. (2019), denoted as “Box-Cox”;
- the method in Zhou and Lin (2008) under the binormal model, denoted as “ZL”;
- the method in Lin et al. (2012), denoted as “LZL”;
- the ECDF-based method, denoted as “ECDF”, which is also known as the nonparametric estimator in Pepe (2003) and Zhou et al. (2011);
- the maximum nonparametric likelihood method under the likelihood ratio ordering (Dykstra et al., 1995), denoted as “MNLE”;
- the kernel-based method in Bantis et al. (2019), denoted as “Kernel”;
- the maximum smoothed likelihood method under the likelihood ratio ordering in Yu et al. (2017), denoted as “MSLE”.

In the Kernel and MSLE methods, we follow Bantis et al. (2019) and Yu et al. (2017). We use the Gaussian kernel with bandwidths h_0 and h_1 for healthy and diseased groups respectively, where

$$h_0 = 0.9 \min \left\{ s_0, \frac{q_0}{1.34} \right\} n_0^{-0.2} \quad \text{and} \quad h_1 = 0.9 \min \left\{ s_1, \frac{q_1}{1.34} \right\} n_1^{-0.2}.$$

Here, s_0 and q_0 are sample standard deviation and sample interquartile range for the sample from the healthy population, and s_1 and q_1 are sample standard deviation and sample interquartile range for the sample from the diseased population.

Throughout our numerical studies, we observe that the MNLE and MSLE methods have similar performance as that of the ECDF and kernel methods, respectively. Furthermore, the LZL method is designed to accommodate covariates; without covariates, the performance of this method is very similar to that of the ECDF method. For space limitation, we present the results for MNLE, MSLE, and LZL methods in the supplementary material.

We consider two distributional settings:

- (1) $f_0 \sim N(\mu_0, \sigma_0^2)$ and $f_1 \sim N(\mu_1, \sigma_1^2)$;
- (2) $f_0 \sim \text{Gamma}(a_0, b_0)$ and $f_1 \sim \text{Gamma}(a_1, b_1)$.

Here, $\text{Gamma}(a, b)$ denotes the gamma distribution with shape parameter a and rate parameter b . Note that Setting (1) corresponds to the case that the model assumption for the Box-Cox method is satisfied, whereas Setting (2) corresponds to the case that the model assumption for the Box-Cox method is violated. In both cases, f_0 is fixed. The parameters for f_1 are varied such that the corresponding Youden indices are 0.3, 0.5, and 0.7, respectively. The details of these settings are given in Table 1. We consider three different combinations of sample sizes: $(n_0, n_1) = (50, 50)$, $(100, 100)$, and $(150, 50)$. Therefore, for each distributional setting of f_0 and f_1 , we have 9 combinations of parameters and sample sizes. For each combination, we repeat the simulation 2000 times.

We observe that the proposed method depends on the choice of N . In the supplementary material, we give the frequency of the selected N values based on the BIC criterion given in Remark 1 from 2000 repetitions. Furthermore, we have considered the distributional setting that f_0 and f_1 follow the Beta distributions; the details and results are also given in the supplementary material.

Table 1: Simulation settings

Distribution	J	AUC	μ_0	σ_0^2	μ_1	σ_1^2
Normal	0.3	0.707	10	1	10.771	1
Normal	0.5	0.830	10	1	11.349	1
Normal	0.7	0.929	10	1	12.073	1
Distribution	J	AUC	a_0	b_0	a_1	b_1
Gamma	0.3	0.708	2	1	3	0.937
Gamma	0.5	0.830	2	1	4	0.944
Gamma	0.7	0.929	2	1	5	0.827

3.2 Comparison of the ROC curve estimation

In this section, we compare our proposed method with the competitive methods in the ROC curve estimation. The criteria for comparison are the L_1 - and L_2 -distances between the estimated and the true ROC curves. For a generic ROC curve estimate $\overline{ROC}(s)$, the L_1 - and L_2 -distances between $\overline{ROC}(s)$ and the true ROC curve $ROC(s)$ are defined to be:

$$L_1(\overline{ROC}, ROC) = \int_0^1 |\overline{ROC}(s) - ROC(s)| ds$$

and

$$L_2(\overline{ROC}, ROC) = \left[\int_0^1 \{\overline{ROC}(s) - ROC(s)\}^2 ds \right]^{1/2}.$$

Simulation results based on 2000 repetitions are summarized in Table 2.

From this table and the results given in the supplementary material, we observe that our BP method results in the smallest average L_1 - and L_2 -distances for all the examples; the improvement is significant. For example, the ratio of the L_2 -distances between our BP method and the ECDF method is ranged between 0.61 and 0.71 with an average of 0.66; the ratio of the L_2 -distances between our BP method and the ZL method is between 0.84 and 0.93 with an average of 0.88.

3.3 Comparison of the AUC estimation

In this section, we compare our proposed method with the competitive methods in the AUC estimation. The criteria for comparison are the relative bias (RB) and mean square error (MSE). Suppose we have B point estimates of the AUC $\hat{a}^{(i)}$ for $i = 1, \dots, B$. The RB in percentage and the MSE are respectively defined to be:

$$RB(\%) = \frac{1}{B} \sum_{i=1}^B \frac{\hat{a}^{(i)} - a_0}{a_0} \times 100 \quad \text{and} \quad MSE = \frac{1}{B} \sum_{i=1}^B (\hat{a}^{(i)} - a_0)^2,$$

where a_0 is the true value of the AUC. The results are summarized in Table 3.

Comparing the RB values in this table, we observe that our method is small in RB values for all examples, though in most cases, the RB values from the ECDF method are the smallest; the kernel method always results in negative and largest RBs in absolute values. Comparing the MSE values, our BP method has comparable or better performance than competitive methods.

3.4 Comparison of the Youden index and optimal cutoff point estimation

In this section, we compare our method with the competitive methods in the estimation of the Youden index and the optimal cutoff point. The criteria for comparison are the RB and MSE, which are similarly

Table 2: Averages of L_1 -distances and L_2 -distances of five methods for estimating the ROC curve

Distribution (J)	(n_0, n_1) Method	(50, 50)		(100, 100)		(150, 50)	
		L_1	L_2	L_1	L_2	L_1	L_2
Normal (0.3)	BP	0.040	0.046	0.029	0.033	0.033	0.038
	Box-Cox	0.044	0.053	0.032	0.038	0.037	0.043
	ZL	0.045	0.054	0.032	0.038	0.037	0.044
	ECDF	0.056	0.071	0.040	0.051	0.046	0.058
	Kernel	0.047	0.057	0.035	0.042	0.040	0.048
Normal (0.5)	BP	0.032	0.041	0.023	0.029	0.026	0.034
	Box-Cox	0.036	0.047	0.025	0.034	0.029	0.038
	ZL	0.036	0.049	0.026	0.034	0.030	0.039
	ECDF	0.045	0.064	0.032	0.046	0.037	0.051
	Kernel	0.040	0.053	0.029	0.040	0.033	0.043
Normal (0.7)	BP	0.020	0.033	0.014	0.023	0.016	0.026
	Box-Cox	0.022	0.036	0.015	0.026	0.017	0.028
	ZL	0.023	0.039	0.016	0.027	0.019	0.030
	ECDF	0.029	0.053	0.020	0.038	0.023	0.040
	Kernel	0.027	0.044	0.020	0.033	0.022	0.035
Gamma (0.3)	BP	0.042	0.050	0.030	0.035	0.035	0.041
	Box-Cox	0.045	0.054	0.032	0.038	0.037	0.044
	ZL	0.047	0.056	0.032	0.039	0.038	0.045
	ECDF	0.057	0.072	0.040	0.052	0.046	0.058
	Kernel	0.051	0.062	0.038	0.046	0.044	0.051
Gamma (0.5)	BP	0.034	0.046	0.024	0.032	0.027	0.035
	Box-Cox	0.036	0.049	0.026	0.035	0.028	0.037
	ZL	0.037	0.050	0.026	0.035	0.028	0.038
	ECDF	0.045	0.067	0.032	0.047	0.036	0.050
	Kernel	0.046	0.060	0.035	0.044	0.038	0.046
Gamma (0.7)	BP	0.021	0.036	0.016	0.026	0.016	0.027
	Box-Cox	0.022	0.038	0.016	0.027	0.016	0.028
	ZL	0.023	0.040	0.016	0.028	0.018	0.031
	ECDF	0.029	0.055	0.021	0.040	0.022	0.040
	Kernel	0.033	0.050	0.026	0.038	0.028	0.038

Table 3: RB (%) and MSE ($\times 1000$) of five methods for estimating the AUC

Distribution (J)	(n_0, n_1) Method	(50, 50)		(100, 100)		(150, 50)	
		RB	MSE	RB	MSE	RB	MSE
Normal (0.3)	BP	0.29	2.39	0.00	1.21	0.20	1.65
	Box-Cox	0.44	2.44	0.06	1.23	0.20	1.68
	ZL	0.44	2.47	0.09	1.24	0.24	1.69
	ECDF	0.09	2.51	-0.10	1.27	-0.01	1.74
	Kernel	-1.67	2.38	-1.54	1.28	-1.53	1.71
Normal (0.5)	BP	0.16	1.50	-0.01	0.75	0.16	1.01
	Box-Cox	0.35	1.50	0.08	0.75	0.17	1.02
	ZL	0.36	1.53	0.10	0.76	0.19	1.03
	ECDF	0.03	1.56	-0.07	0.77	-0.01	1.06
	Kernel	-1.95	1.77	-1.68	0.95	-1.71	1.24
Normal (0.7)	BP	0.05	0.58	-0.01	0.28	0.08	0.37
	Box-Cox	0.10	0.54	0.01	0.27	0.05	0.36
	ZL	0.14	0.58	0.04	0.28	0.10	0.40
	ECDF	-0.02	0.61	-0.04	0.29	-0.01	0.39
	Kernel	-1.56	0.88	-1.28	0.46	-1.33	0.59
Gamma (0.3)	BP	0.69	2.49	0.29	1.26	0.11	1.70
	Box-Cox	0.57	2.58	0.26	1.30	0.23	1.76
	ZL	0.55	2.60	0.24	1.30	0.20	1.75
	ECDF	0.04	2.66	-0.08	1.34	-0.10	1.78
	Kernel	-2.36	2.63	-2.08	1.44	-2.28	1.86
Gamma (0.5)	BP	0.33	1.56	0.06	0.80	0.17	0.94
	Box-Cox	0.40	1.55	0.13	0.80	0.39	0.95
	ZL	0.39	1.58	0.10	0.81	0.36	0.97
	ECDF	-0.01	1.65	-0.14	0.84	0.13	0.99
	Kernel	-2.65	2.12	-2.31	1.20	-2.33	1.37
Gamma (0.7)	BP	0.10	0.59	-0.01	0.30	0.00	0.35
	Box-Cox	0.08	0.55	-0.01	0.29	0.08	0.32
	ZL	0.13	0.59	-0.01	0.30	0.14	0.39
	ECDF	-0.05	0.62	-0.10	0.31	0.00	0.35
	Kernel	-2.19	1.14	-1.82	0.65	-2.03	0.80

defined as those in Section 3.3. The simulation results for estimating the Youden index and the optimal cutoff point are summarized in Tables 4 and 5, respectively.

From Table 4, we observe that in the estimation of the Youden index, out of 18 simulation settings, our BP method leads to the smallest RB values in 16 settings, and obtains the second smallest RB values in 2 settings, where the kernel method produces the smallest RB values. Comparing MSE values, the performance of our BP method and the Box-Cox method is comparable, and is better than the other methods in most of the settings.

From Table 5, for estimating the cutoff point, our BP method and the Box-Cox method result in significantly smaller MSE values than other methods. The performance of the BP and the Box-Cox method is mixed. When f_0 and f_1 are simulated from the Gamma distribution and the Youden index is 0.7, Box-Cox method produces smaller MSE values, whereas our BP method leads to smaller MSE values in all other settings.

4 Real data application

In this section, we apply our method to a dataset on Duchenne Muscular Dystrophy (DMD). DMD is a type of muscular dystrophy that is genetically transmitted from a mother to her children. Muscle loss occurs at an early age for offspring with the disease. Female offspring with the disease do not suffer from significant symptoms compared to male offspring who die at a young age. Female carriers do not show sign of disease and therefore detection of potential female carrier is of main interest.

Percy et al. (1982) stated that DMD carriers are more likely to have higher measurement of specific biomarkers. Four biomarkers including creatine kinase (CK), hemopexin (H), lactate dehydrogenase (LD), and pyruvate kinase (PK) are measured from the blood serum samples of a healthy group ($n_0 = 127$) and a group of carriers ($n_1 = 67$). The complete dataset was collected by Andrews and Herzberg (2012). Yuan et al. (2021) pointed out that the biomarker CK has the best performance among these four biomarkers since it corresponds to largest estimate of the Youden index. Therefore, we apply our method and other existing methods on the biomarker CK to compare their performance.

Following Remark 1, we construct the $BIC(N)$ versus N plot in Panel (a) of Figure 1; it suggests to use $N = 1$ in our BP method. Based on Remark 4, to check whether the likelihood ratio ordering assumption is reasonable, we plot our BP estimates (\hat{F}_0, \hat{F}_1) and the empirical cdf estimates $(\tilde{F}_0, \tilde{F}_1)$ in Panel (b) of Figure 1; this plot suggests that the likelihood ratio ordering assumption might be reasonable. We further perform the goodness-of-fit test suggested in Remark 4; the p -value based on 1000 bootstrap sample is 0.975. This reinforces the validity of the likelihood ratio ordering assumption.

In Figure 2, we plot the ROC curve estimates from our BP and competitive methods. The performance of the MNLE and MSLE methods is similar to that of the ECDF and kernel method, respectively; we thus do not include them in this figure. From the figure, we observe that the ROC curve estimate from our BP method is similar to those of Box-Cox, ZL, ECDF, and LZL methods, but different from the kernel method. The difference lies in the fact that the kernel method leads to much smaller sensitivity estimate compared to other methods when 1-specificity is large, greater than 0.5 say. This is mainly because that the CK values for the diseased individuals are very skewed, which inflates the selected bandwidth when the kernel method is used to estimate F_1 ; this in turn makes F_1 overestimated and hence causes the sensitivity underestimated when 1-specificity is large or the value of CK is small.

We evaluate the point estimates (PEs) and bootstrap percentile confidence intervals (BPCIs) of the AUC, Youden index, and optimal cutoff point based on different methods, and display them in Table 6. The AUC estimates from all methods are similar, except for the kernel method, which leads to a smaller AUC estimate. This is consistent with the results in Figure 2, and complies with our observation in Table 3: the kernel method has the negative relative biases, and all other methods have small RBs and comparable MSEs. The Youden index estimates are similar for all methods: the maximum difference between any two estimates is less than 0.03. For the optimal cutoff point estimates, the kernel method leads to a different result from other methods; other methods give similar results. But the ZL, LZL and ECDF methods have resulted in wider BPCIs than our method; we conjecture that this may indicate that our method has given smaller standard error than other methods in the optimal cutoff point estimation.

Table 4: RB (%) and MSE ($\times 1000$) of five methods for estimating the Youden index

Distribution (J)	(n_0, n_1) Method	$(50, 50)$		$(100, 100)$		$(150, 50)$	
		RB	MSE	RB	MSE	RB	MSE
Normal (0.3)	BP	1.90	5.69	0.44	2.87	1.25	3.93
	Box-Cox	4.25	5.86	1.57	2.89	2.50	3.97
	ZL	4.66	5.94	1.80	2.92	2.84	4.01
	ECDF	24.05	11.64	11.57	5.57	19.05	7.75
	Kernel	-0.88	5.61	-2.53	3.08	-1.83	4.05
Normal (0.5)	BP	1.32	4.91	0.40	2.43	0.99	3.29
	Box-Cox	2.64	5.04	1.05	2.42	1.52	3.33
	ZL	2.89	5.24	1.15	2.47	1.70	3.40
	ECDF	11.67	9.15	7.40	4.33	9.28	6.13
	Kernel	-3.53	5.45	-3.73	3.01	-3.54	3.90
Normal (0.7)	BP	1.01	3.51	0.37	1.68	0.74	2.25
	Box-Cox	1.64	3.38	0.70	1.61	0.95	2.20
	ZL	2.09	3.84	0.89	1.77	1.40	2.87
	ECDF	6.29	5.71	4.06	2.79	5.01	3.80
	Kernel	-3.74	4.43	-3.43	2.43	-3.43	3.10
Gamma (0.3)	BP	3.85	6.03	1.74	2.98	1.32	4.03
	Box-Cox	5.27	6.25	2.90	3.08	3.18	4.27
	ZL	5.60	6.32	2.92	3.08	3.19	4.23
	ECDF	23.77	11.66	15.77	5.83	19.08	7.85
	Kernel	-0.67	6.10	-1.91	3.35	-0.95	4.17
Gamma (0.5)	BP	1.92	5.27	0.57	2.56	1.08	3.09
	Box-Cox	3.26	5.33	1.66	2.58	2.62	3.33
	ZL	3.30	5.47	1.54	2.60	2.43	3.35
	ECDF	11.20	9.02	7.25	4.45	9.38	5.94
	Kernel	-3.42	5.91	-3.64	3.21	-2.96	3.55
Gamma (0.7)	BP	1.34	3.66	0.51	1.83	0.71	2.09
	Box-Cox	1.88	3.46	0.95	1.75	1.37	2.08
	ZL	2.28	4.03	1.01	1.89	1.81	3.26
	ECDF	6.17	5.87	3.85	2.86	4.95	3.62
	Kernel	-3.71	4.56	-3.50	2.62	-3.62	2.88

Table 5: RB (%) and MSE ($\times 1000$) of five methods for estimating the optimal cutoff point

Distribution (J)	(n_0, n_1) Method	(50, 50)		(100, 100)		(150, 50)	
		RB	MSE	RB	MSE	RB	MSE
Normal (0.3)	BP	-0.19	11.34	-0.18	5.72	-0.17	7.60
	Box-Cox	-0.11	44.14	-0.02	22.61	-0.08	29.02
	ZL	-0.22	58.06	-0.04	27.42	-0.05	35.82
	ECDF	-0.14	137.99	-0.13	95.68	0.15	114.03
	Kernel	0.04	110.52	0.06	64.31	0.28	79.47
Normal (0.5)	BP	-0.15	11.40	-0.13	5.70	-0.11	7.51
	Box-Cox	-0.09	22.44	-0.02	11.15	-0.03	13.51
	ZL	-0.22	33.61	-0.06	15.88	0.00	19.40
	ECDF	-0.22	82.58	-0.10	56.55	-0.14	68.46
	Kernel	-0.03	42.51	-0.04	23.82	0.09	30.02
Normal (0.7)	BP	-0.11	12.96	-0.10	6.37	-0.05	8.44
	Box-Cox	-0.06	15.56	-0.02	7.48	0.01	9.23
	ZL	-0.23	31.01	-0.08	14.66	-0.01	18.19
	ECDF	-0.27	62.74	-0.10	38.93	0.13	51.15
	Kernel	-0.04	27.67	0.01	14.65	0.03	19.03
Gamma (0.3)	BP	4.48	58.33	2.96	31.53	3.67	42.28
	Box-Cox	0.21	88.72	-0.38	43.95	-0.42	52.51
	ZL	0.44	120.92	-0.12	56.77	0.67	71.78
	ECDF	2.86	319.78	1.78	206.42	4.09	274.15
	Kernel	12.12	307.63	8.73	150.92	10.95	189.00
Gamma (0.5)	BP	2.69	45.48	1.98	24.47	2.48	32.88
	Box-Cox	-0.46	52.60	-0.42	27.26	-0.27	30.60
	ZL	-0.39	81.87	-0.07	39.84	0.87	47.04
	ECDF	0.01	210.50	0.62	144.56	2.08	181.49
	Kernel	7.17	141.60	5.72	80.26	6.97	94.56
Gamma (0.7)	BP	1.53	57.16	1.15	31.92	1.53	41.74
	Box-Cox	-0.62	51.57	-0.57	26.03	-0.42	32.98
	ZL	-0.59	106.81	-0.24	53.14	0.39	66.29
	ECDF	-0.59	223.80	-0.12	150.58	1.27	193.70
	Kernel	4.38	140.67	3.56	75.42	4.03	82.75

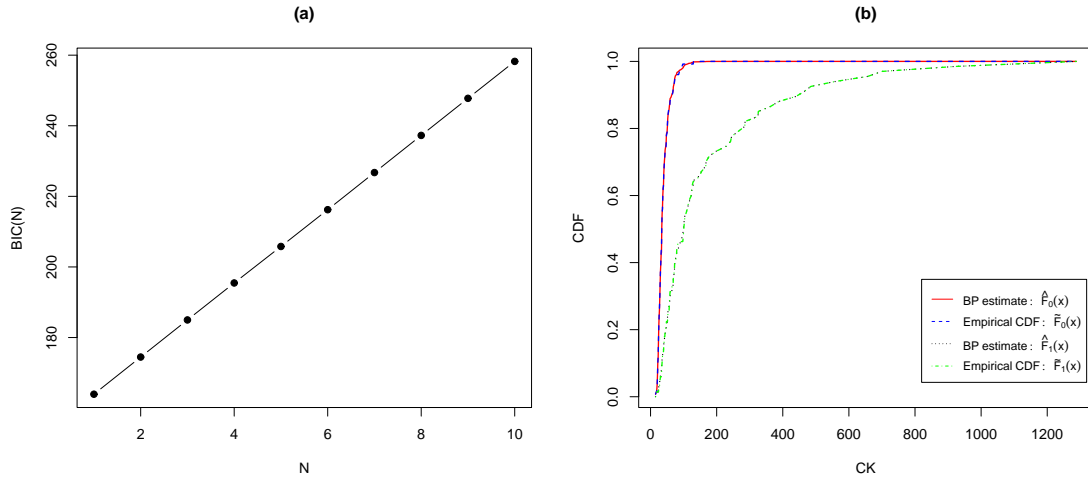


Figure 1: Panel (a) shows $BIC(N)$ versus N ; Panel (b) compares the proposed estimators (\hat{F}_0, \hat{F}_1) and the empirical cdfs (\tilde{F}_0, \tilde{F}_1).

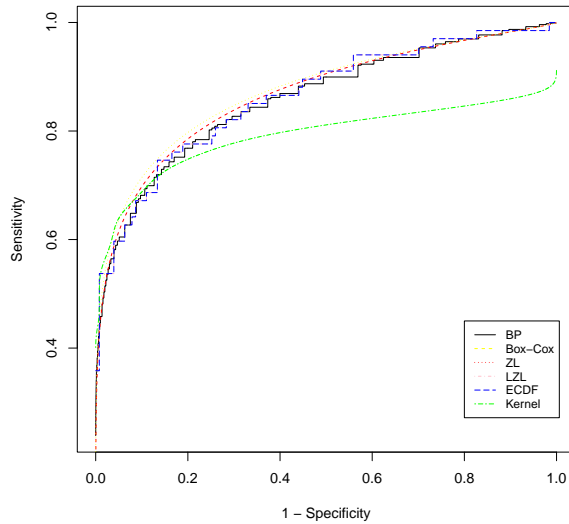


Figure 2: Estimated ROC curves based on different methods.

However, unlike with the simulation studies, in this real data example, we are unable to compare the estimates with the true values.

5 Conclusion

We have proposed a Bernstein polynomial method to estimate the cdfs of the biomarkers in the two-sample problem under the likelihood ratio ordering assumption, and subsequently considered the the

Table 6: PEs and BPCIs of the AUC, Youden index, and optimal cutoff point by using CK as the biomarker

Statistics	AUC		Youden index		Optimal cutoff point	
Method	PE	BPCI	PE	BPCI	PE	BPCI
BP	0.865	[0.804, 0.914]	0.588	[0.480, 0.688]	58.998	[51.976, 67.311]
Box-Cox	0.874	[0.816, 0.921]	0.616	[0.510, 0.710]	58.017	[51.869, 65.055]
ZL	0.868	[0.805, 0.917]	0.600	[0.498, 0.697]	57.000	[50.975, 69.000]
LZL	0.863	[0.800, 0.914]	0.612	[0.502, 0.727]	56.000	[43.000, 97.500]
ECDF	0.863	[0.800, 0.914]	0.612	[0.502, 0.727]	56.000	[43.000, 97.500]
Kernel	0.790	[0.748, 0.844]	0.591	[0.502, 0.669]	73.356	[54.689, 79.413]

estimation of the ROC curve and its summary statistics. With simulation studies, we have compared our method with existing methods; we observe that our method performs well in the estimation of both the ROC curve and the summary statistics. With the empirical process theory, we established the consistency of our estimators. We implemented the numerical algorithm for our method in an R package named BPLR, which is ready to be applied in practice.

We observe that within the framework of this article, there are many interesting topics that can be explored in the future. First, we have established the consistency of our proposed estimators, but not the convergence rates and the asymptotic distributions; if we are able to establish the asymptotic distributions of them in the future, we can construct the confidence bands/intervals for $F_0(\cdot)$, $F_1(\cdot)$, $ROC(\cdot)$, and other summary statistics. Second, we have proposed to employ the Youden index as the criterion, and maximise it to determine the optimal cutoff point; however, there may exist other criteria; for example, the closest to (0,1) criterion and equal sensitivity and specificity criterion (Sande et al., 2021). It could be interesting to explore how to extend our method to accommodate these criteria. Third, in Remark 3, we have suggested to include the log transformed biomarker in our model and have applied this strategy in both the simulation and real data analysis. We observe that there may exist other reasonable transformations that can be incorporated in our method, for example, Yang et al. (2021) proposed a transformation method based on the likelihood ratio and discussed the scenarios under which that transformation is applicable. We leave this for future research.

Appendix: Regularity Conditions

We need the following conditions in our technical developments for Theorems 1 and 2. They are not necessarily the weakest possible.

- A1 The total sample size $n = n_0 + n_1 \rightarrow \infty$ and $n_1/n \rightarrow \lambda$ for $\lambda \in (0, 1)$ being a constant.
- A2 The order $N \rightarrow \infty$ as $n \rightarrow \infty$ and $\lim_{n \rightarrow \infty} N/n = 0$.
- A3 The likelihood ratio ordering assumption is satisfied, or equivalently, $\theta_0(x)$ in (14) is a nondecreasing function of x . Furthermore, $\theta_0(x)$ is a continuous function of x and there exists a $\delta > 0$ such that $\delta \leq \theta_0(x) \leq 1 - \delta$ for all $x \in [0, 1]$.
- A4 There exists an $\epsilon_0 > 0$, such that $\theta_0(x)$ is strictly increasing for $x \in [C - \epsilon_0, C + \epsilon_0]$, where C is defined by (11).

References

- Andrews, D. F. and A. M. Herzberg (2012). *Data: A Collection of Problems from Many Fields for the Student and Research Worker*. New York: Springer.
- Bantis, L. E., C. T. Nakas, and B. Reiser (2019). Construction of confidence intervals for the maximum of the youden index and the corresponding cutoff point of a continuous biomarker. *Biometrical Journal* 61, 138–156.
- Chen, B., P. Li, J. Qin, and T. Yu (2016). Using a monotonic density ratio model to find the asymptotically optimal combination of multiple diagnostic tests. *Journal of the American Statistical Association* 111, 861–874.
- Dykstra, R., S. Kocher, and T. Robertson (1995). Inference for likelihood ratio ordering in the two-sample problem. *Journal of the American Statistical Association* 90, 1034–1040.
- Friedman, J., T. Hastie, and R. Tibshirani (2010). Regularization paths for generalized linear models via coordinate descent. *Journal of Statistical Software* 33, 1–22.
- Gneiting, T. and P. Vogel (2018). Receiver operating characteristic (roc) curves. *arXiv preprint arXiv:1809.04808*.
- Jokiel-Rokita, A. and M. Pulit (2013). Nonparametric estimation of the roc curve based on smoothed empirical distribution functions. *Statistics and Computing* 23, 703–712.
- Kosorok, M. R. (2008). *Introduction to Empirical Processes and Semiparametric Inference*. New York: Springer.
- Lin, H., X.-H. Zhou, and G. Li (2012). A direct semiparametric receiver operating characteristic curve regression with unknown link and baseline functions. *Statistica Sinica* 22, 1427–1456.
- Lorentz, G. G. (1986). *Bernstein Polynomials* (Second ed.). New York: Chelsea Publishing Company.
- Owen, A. B. (2001). *Empirical Likelihood*. New York: Chapman and Hall/CRC.
- Pepe, M. S. (2003). *The Statistical Evaluation of Medical Tests for Classification and Prediction*. New York: Oxford University Press.
- Percy, M. E., D. F. Andrews, and M. W. Thompson (1982). Duchenne muscular dystrophy carrier detection using logistic discrimination: Serum creatine kinase, hemopexin, pyruvate kinase, and lactate dehydrogenase in combination. *American Journal of Medical Genetics* 13, 27–38.
- Qin, J. and B. Zhang (2003). Using logistic regression procedures for estimating receiver operating characteristic curves. *Biometrika* 90, 585–596.
- Sande, S. Z., L. Seng, J. Li, and R. D’Agostino (2021). Statistical learning in medical research with decision threshold and accuracy evaluation. *Journal of Data Science* 19, 634–657.
- Wang, D., L. Tian, and Y. Zhao (2017). Smoothed empirical likelihood for the youden index. *Computational Statistics & Data Analysis* 115, 1–10.
- Wang, J. and S. Ghosh (2012). Shape restricted nonparametric regression with bernstein polynomials. *Computational Statistics & Data Analysis* 56, 2729–2741.
- Yang, J., P.-F. Kuan, and J. Li (2021). Transformation based on likelihood ratio. *Statistical Methods in Medical Research* 30, 354–356.

- Yin, J. and L. Tian (2014). Joint inference about sensitivity and specificity at the optimal cut-off point associated with youden index. *Computational Statistics & Data Analysis* 77, 1–13.
- Youden, W. J. (1950). Index for rating diagnostic tests. *Cancer* 3, 32–35.
- Yu, T., P. Li, and J. Qin (2017). Density estimation in the two-sample problem with likelihood ratio ordering. *Biometrika* 104, 141–152.
- Yuan, M., P. Li, and C. Wu (2021). Semiparametric inference of the youden index and the optimal cut-off point under density ratio models. *The Canadian Journal of Statistics* 49, 965–986.
- Zhou, X., D. K. McClish, and N. A. Obuchowski (2011). *Statistical Methods in Diagnostic Medicine* (Second ed.). New York: Wiley.
- Zhou, X.-H. and H. Lin (2008). Semi-parametric maximum likelihood estimates for roc curves of continuous-scale tests. *Statistics in Medicine* 27, 5271–5290.

Supplementary Material for “Statistical inference for the two-sample problem under likelihood ratio ordering, with application to the ROC curve estimation”

Abstract

This is a supplementary document to the paper “Statistical inference for the two-sample problem under likelihood ratio ordering, with application to the ROC curve estimation”. Section S1 gives some additional simulation results. Section S2 proves Proposition 1 in the main article. Sections S3 and S4 present technical details for Theorems 1 and 2 in the main article.

S1 Additional simulation results

S1.1 Additional simulation results when f_0 and f_1 are from the normal and Gamma distributions

In this section, we first present the frequency of the selected N values based on the BIC criterion in Remark 1 of the main article; the results are given in Table S1. Based on Remark 3 of the main article, we include both the original and log-transformed biomarkers in the model. Hence, for both normal and Gamma distributions, the true value of N is 1. From Table S1, we observe that the proposed BIC criterion can choose $N = 1$ for the majority of repetitions in all the simulation settings.

Tables S2–S5 summarize the results of the maximum nonparametric likelihood method (MNLE), the maximum smoothed likelihood method (MSLE), and the method in Lin et al. (2012) (LZL) in the estimation of the receiver operating characteristic (ROC) curve, the area under the curve (AUC), the Youden index, and the optimal cutoff point. From these tables, we observe that the performance of MNLE is similar to that of the empirical cumulative distribution function (ECDF) based method; the performance of the MSLE is close to that of the kernel method. The results of LZL are very similar to those of the ECDF method.

Table S1: Frequency of the N values when distributions are normal and Gamma

Distribution (J)	$(n_0, n_1) = (50, 50)$			$(n_0, n_1) = (100, 100)$			$(n_0, n_1) = (150, 50)$		
	$N = 1$	$N = 2$	$N = 3$	$N = 1$	$N = 2$	$N = 3$	$N = 1$	$N = 2$	$N = 3$
Normal (0.3)	1994	6	0	1999	1	0	1995	5	0
Normal (0.5)	1999	1	0	1999	1	0	1999	1	0
Normal (0.7)	2000	0	0	2000	0	0	2000	0	0
Gamma (0.3)	1982	18	0	1986	14	0	1995	5	0
Gamma (0.5)	1988	12	0	1991	9	0	1992	8	0
Gamma (0.7)	1996	4	0	2000	0	0	2000	0	0

Table S2: Averages of L_1 - and L_2 -distances of the ROC curve estimates

Distribution (J)	(n_0, n_1) Method	(50, 50)		(100, 100)		(150, 50)	
		L_1	L_2	L_1	L_2	L_1	L_2
Normal (0.3)	MNLE	0.054	0.066	0.038	0.047	0.045	0.054
	MSLE	0.045	0.054	0.035	0.041	0.039	0.046
	LZL	0.056	0.071	0.040	0.051	0.046	0.058
Normal (0.5)	MNLE	0.042	0.059	0.030	0.043	0.035	0.047
	MSLE	0.039	0.052	0.029	0.039	0.033	0.043
	LZL	0.045	0.064	0.032	0.046	0.037	0.051
Normal (0.7)	MNLE	0.026	0.047	0.019	0.035	0.021	0.036
	MSLE	0.027	0.044	0.020	0.033	0.022	0.035
	LZL	0.029	0.053	0.020	0.038	0.023	0.040
Gamma (0.3)	MNLE	0.054	0.067	0.039	0.048	0.044	0.054
	MSLE	0.049	0.059	0.037	0.044	0.042	0.049
	LZL	0.057	0.072	0.040	0.052	0.046	0.058
Gamma (0.5)	MNLE	0.042	0.061	0.031	0.044	0.034	0.047
	MSLE	0.045	0.058	0.034	0.044	0.037	0.046
	LZL	0.045	0.067	0.032	0.047	0.036	0.050
Gamma (0.7)	MNLE	0.025	0.049	0.019	0.036	0.020	0.036
	MSLE	0.033	0.049	0.025	0.037	0.027	0.038
	LZL	0.029	0.055	0.021	0.040	0.022	0.040

Table S3: RB (%) and MSE ($\times 1000$) of the AUC estimates

Distribution (J)	(n_0, n_1) Method	(50, 50)		(100, 100)		(150, 50)	
		RB	MSE	RB	MSE	RB	MSE
Normal (0.3)	MNLE	5.09	3.39	3.39	1.69	4.17	2.35
	MSLE	-1.35	2.23	-1.41	1.24	-1.33	1.63
	LZL	0.09	2.51	-0.10	1.27	-0.01	1.74
Normal (0.5)	MNLE	2.90	1.88	1.95	0.94	2.37	1.29
	MSLE	-1.88	1.75	-1.66	0.95	-1.67	1.23
	LZL	0.03	1.56	-0.07	0.77	-0.01	1.06
Normal (0.7)	MNLE	1.40	0.63	1.00	0.33	1.18	0.43
	MSLE	-1.54	0.87	-1.27	0.46	1.31	0.59
	LZL	-0.02	0.61	-0.04	0.29	-0.01	0.39
Gamma (0.3)	MNLE	5.04	3.47	3.40	1.77	4.04	2.34
	MSLE	-1.88	2.43	-1.85	1.38	-1.96	1.75
	LZL	0.05	2.66	-0.08	1.35	-0.10	1.78
Gamma (0.5)	MNLE	2.85	1.92	1.88	0.99	2.43	1.25
	MSLE	-2.48	2.04	-2.22	1.17	-2.23	1.33
	LZL	-0.01	1.65	-0.14	0.84	0.13	0.99
Gamma (0.7)	MNLE	1.35	0.63	0.94	0.34	1.14	0.40
	MSLE	-2.10	1.11	-1.77	0.63	-1.98	0.78
	LZL	-0.05	0.62	-0.10	0.31	0.00	0.35

Table S4: RB (%) and MSE ($\times 1000$) of the Youden index estimates

Distribution (J)	(n_0, n_1) Method	(50, 50)		(100, 100)		(150, 50)	
		L_1	L_2	L_1	L_2	L_1	L_2
Normal (0.3)	MNLE	24.05	11.64	11.57	5.57	19.05	7.75
	MSLE	-0.88	5.61	-2.53	3.08	-1.83	4.05
	LZL	24.04	11.63	15.55	5.57	19.03	7.75
Normal (0.5)	MNLE	11.67	9.15	7.40	4.33	9.28	6.13
	MSLE	-3.53	5.45	-3.73	3.01	-3.54	3.90
	LZL	11.66	9.15	7.39	4.33	9.27	6.12
Normal (0.7)	MNLE	6.29	5.71	4.06	2.79	5.01	3.80
	MSLE	-3.74	4.43	-3.43	2.43	-3.43	3.10
	LZL	6.28	5.70	4.06	2.79	5.00	3.79
Gamma (0.3)	MNLE	23.77	11.66	15.77	5.83	19.08	7.85
	MSLE	-0.67	6.10	-1.91	3.35	-0.95	4.17
	LZL	23.76	11.65	15.75	5.82	19.07	7.84
Gamma (0.5)	MNLE	11.20	9.02	7.25	4.45	9.38	5.94
	MSLE	-3.42	5.91	-3.64	3.21	-2.96	3.55
	LZL	11.19	9.01	7.24	4.45	9.37	5.94
Gamma (0.7)	MNLE	6.17	5.87	3.85	2.86	4.95	3.62
	MSLE	-3.71	4.56	-3.50	2.62	-3.62	2.88
	LZL	6.16	5.87	3.85	2.86	4.95	3.62

Table S5: RB (%) and MSE ($\times 1000$) of the optimal cutoff point estimates

Distribution (J)	(n_0, n_1) Method	(50, 50)		(100, 100)		(150, 50)	
		RB	MSE	RB	MSE	RB	MSE
Normal (0.3)	MNLE	-0.13	137.31	-0.13	95.25	0.14	113.75
	MSLE	0.04	110.52	-0.06	64.32	0.28	79.45
	LZL	-0.17	146.41	-0.10	100.75	0.16	118.25
Normal (0.5)	MNLE	-0.22	82.46	-0.10	56.07	-0.14	68.40
	MSLE	-0.04	42.52	-0.04	23.82	0.08	30.02
	LZL	-0.25	87.21	-0.12	59.57	0.13	70.82
Normal (0.7)	MNLE	-0.26	62.73	-0.09	38.80	0.13	51.15
	MSLE	-0.05	27.67	0.00	14.65	0.02	19.03
	LZL	-0.29	64.95	-0.08	40.22	0.15	52.01
Gamma (0.3)	MNLE	2.67	313.56	1.65	204.17	4.00	272.66
	MSLE	12.10	307.44	8.71	150.78	10.93	188.82
	LZL	2.81	341.48	1.94	218.63	4.09	284.06
Gamma (0.5)	MNLE	-0.03	209.13	0.60	144.27	2.03	180.81
	MSLE	7.16	141.44	5.70	80.14	6.95	94.40
	LZL	-0.14	227.38	0.49	149.22	3.86	211.86
Gamma (0.7)	MNLE	-0.62	222.60	-0.12	149.71	1.22	192.81
	MSLE	4.36	140.51	3.54	75.29	4.01	82.60
	LZL	-0.70	228.96	0.08	156.61	1.41	198.65

S1.2 Simulation results when f_0 and f_1 follow the Beta distribution

In this section, we consider the simulation when $f_0 \sim \text{Beta}(2, 2)$ and $f_1 \sim \text{Beta}(a_1, b_1)$. For (a_1, b_1) , we consider three sets of values as shown in Table S6 such that the corresponding J is 0.3, 0.5, and 0.7 respectively. We note that under this simulation setup, the true value of N is 1.

Table S7 summarizes the frequency of the selected N values based on the BIC criterion in Remark 1 of the main article; this table shows that the BIC criterion picks the correct order in the majority of the repetitions. Tables S8–S11 summarize the results of all methods for estimating the ROC curve, the AUC, the Youden index, and the optimal cutoff point. The observations are similar to those when f_0 and f_1 are simulated as normal and Gamma distributions; we omit the details. It is noteworthy that the model assumption for the Box-cox method is violated under this setup. Our BP method performs better than the Box-Cox method for estimating the ROC curve, the Youden index, and the optimal cutoff point; the improvement is significant. For estimating the AUC, our BP method leads to smaller MSEs when $J = 0.3$ and 0.5, but the Box-Cox method results in smaller MSEs when $J = 0.7$.

Table S6: Beta simulation setting

Distribution	J	AUC	a_1	b_1
Beta	0.3	0.702	3.838	2
Beta	0.5	0.822	6.148	2
Beta	0.7	0.919	11.014	2

Table S7: Frequency of the chosen N in Beta distributional setting

(n_0, n_1) Distribution (J)	(50, 50)			(100, 100)			(150, 50)		
	$N = 1$	$N = 2$	$N = 3$	$N = 1$	$N = 2$	$N = 3$	$N = 1$	$N = 2$	$N = 3$
Beta (0.3)	1989	11	0	1996	4	0	1998	2	0
Beta (0.5)	1999	1	0	2000	0	0	2000	0	0
Beta (0.7)	2000	0	0	2000	0	0	2000	0	0

Table S8: Averages of L_1 -distances and L_2 -distances of eight methods for estimating the ROC curve

Distribution (J)	(n_0, n_1) Method	$(50, 50)$		$(100, 100)$		$(150, 50)$	
		L_1	L_2	L_1	L_2	L_1	L_2
Beta (0.3)	BP	0.041	0.048	0.029	0.034	0.031	0.037
	Box-Cox	0.045	0.055	0.032	0.039	0.036	0.043
	ZL	0.046	0.057	0.032	0.039	0.035	0.043
	LZL	0.056	0.073	0.040	0.052	0.044	0.057
	ECDF	0.056	0.073	0.040	0.052	0.044	0.057
	MNLE	0.054	0.069	0.039	0.050	0.044	0.055
	Kernel	0.047	0.058	0.034	0.042	0.037	0.046
	MSLE	0.044	0.054	0.034	0.040	0.035	0.044
Beta (0.5)	BP	0.033	0.046	0.024	0.033	0.024	0.033
	Box-Cox	0.039	0.055	0.029	0.041	0.031	0.044
	ZL	0.038	0.054	0.027	0.038	0.027	0.039
	LZL	0.046	0.070	0.032	0.050	0.034	0.051
	ECDF	0.046	0.070	0.032	0.050	0.034	0.051
	MNLE	0.043	0.065	0.032	0.047	0.032	0.047
	Kernel	0.040	0.057	0.029	0.042	0.030	0.042
	MSLE	0.038	0.054	0.028	0.040	0.029	0.041
Beta (0.7)	BP	0.022	0.041	0.015	0.029	0.015	0.028
	Box-Cox	0.028	0.056	0.023	0.046	0.025	0.051
	ZL	0.025	0.050	0.017	0.034	0.020	0.038
	LZL	0.031	0.065	0.021	0.045	0.022	0.044
	ECDF	0.031	0.065	0.021	0.045	0.022	0.044
	MNLE	0.028	0.059	0.020	0.043	0.020	0.041
	Kernel	0.030	0.058	0.022	0.044	0.022	0.042
	MSLE	0.028	0.053	0.021	0.040	0.021	0.039

Table S9: RB (%) and MSE ($\times 1000$) of eight methods for estimating the AUC

Distribution (J)	(n_0, n_1) Method	$(50, 50)$		$(100, 100)$		$(150, 50)$	
		RB	MSE	RB	MSE	RB	MSE
Beta (0.3)	BP	1.07	2.42	0.82	1.20	0.82	1.43
	Box-Cox	1.12	2.72	0.99	1.35	1.17	1.61
	ZL	0.62	2.60	0.50	1.27	0.51	1.51
	LZL	0.14	2.65	0.13	1.31	0.18	1.53
	ECDF	0.14	2.65	0.13	1.31	0.18	1.53
	MNLE	5.33	3.57	3.74	1.82	4.35	2.22
	Kernel	-1.53	2.50	-1.19	1.27	-1.18	1.48
	MSLE	-1.08	2.30	-0.98	1.20	-0.93	1.38
Beta (0.5)	BP	0.66	1.58	0.41	0.81	0.31	0.84
	Box-Cox	1.48	1.74	1.30	0.93	1.16	0.90
	ZL	0.56	1.68	0.32	0.85	0.26	0.87
	LZL	0.13	1.73	0.02	0.87	0.02	0.89
	ECDF	0.13	1.73	0.02	0.87	0.02	0.89
	MNLE	3.16	2.08	2.16	1.08	2.37	1.13
	Kernel	-1.79	1.86	-1.51	0.99	-1.46	1.00
	MSLE	-1.57	1.76	-1.38	0.95	-1.36	0.97
Beta (0.7)	BP	0.36	0.69	0.23	0.33	0.16	0.34
	Box-Cox	0.58	0.60	0.50	0.29	0.09	0.25
	ZL	0.36	0.73	0.20	0.36	0.23	0.83
	LZL	0.11	0.77	0.04	0.37	0.06	0.35
	ECDF	0.11	0.77	0.04	0.37	0.06	0.35
	MNLE	1.70	0.83	1.20	0.43	1.23	0.42
	Kernel	-1.79	1.10	-1.48	0.57	-1.35	0.52
	MSLE	1.56	0.98	-1.34	0.52	-1.23	0.48

Table S10: RB (%) and MSE ($\times 1000$) of eight methods for estimating the Youden index

Distribution (J)	(n_0, n_1) Method	(50, 50)		(100, 100)		(150, 50)	
		RB	MSE	RB	MSE	RB	MSE
Beta (0.3)	BP	4.59	6.07	3.20	2.96	3.36	3.54
	Box-Cox	7.35	7.10	5.75	3.48	3.08	4.65
	ZL	5.76	6.22	3.69	2.96	4.36	3.63
	LZL	23.60	11.63	15.74	5.58	19.37	7.37
	ECDF	23.61	11.64	15.76	5.58	19.39	7.38
	MNLE	23.61	11.64	15.76	5.58	19.39	7.38
	Kernel	0.51	5.98	0.46	3.04	0.00	3.72
	MSLE	0.51	5.98	0.46	3.04	0.00	3.72
Beta (0.5)	BP	2.35	5.23	1.28	2.59	1.08	2.76
	Box-Cox	8.64	7.60	7.34	4.21	8.66	5.13
	ZL	3.86	5.55	2.16	2.64	2.06	2.89
	LZL	11.26	8.78	7.24	4.29	8.78	5.14
	ECDF	11.27	8.78	7.25	4.30	8.79	5.15
	MNLE	11.27	8.78	7.25	4.30	8.79	5.15
	Kernel	-1.29	5.30	-1.69	2.76	-1.71	3.17
	MSLE	-1.29	5.30	-1.69	2.76	-1.71	3.17
Beta (0.7)	BP	1.31	3.67	0.61	1.72	0.51	1.80
	Box-Cox	8.20	6.27	7.60	4.28	7.84	4.65
	ZL	2.71	4.07	1.44	1.86	1.89	4.71
	LZL	6.13	5.84	4.08	2.78	5.03	3.42
	ECDF	6.14	5.84	4.08	2.79	5.03	3.43
	MNLE	6.14	5.84	4.08	2.79	5.03	3.43
	Kernel	-1.39	3.71	-1.47	1.88	-1.20	2.19
	MSLE	-1.39	3.71	-1.47	1.88	-1.20	2.19

Table S11: RB (%) and MSE ($\times 1000$) of eight methods for estimating the optimal cutoff point

Distribution (J)	(n_0, n_1) Method	$(50, 50)$		$(100, 100)$		$(150, 50)$	
		RB	MSE	RB	MSE	RB	MSE
Beta (0.3)	BP	2.18	0.95	2.03	0.61	2.37	0.79
	Box-Cox	-0.41	1.33	-0.30	0.67	-2.03	0.88
	ZL	0.24	2.82	0.71	1.42	0.89	1.81
	LZL	0.97	7.73	1.06	5.59	1.86	6.66
	ECDF	0.97	7.30	1.05	5.25	1.86	6.54
	MNLE	1.10	7.21	1.08	5.22	1.87	6.53
	Kernel	-0.74	5.07	0.44	3.10	-0.14	4.09
	MSLE	-0.74	5.08	-0.45	3.10	-0.14	4.09
Beta (0.5)	BP	1.13	0.62	0.96	0.33	1.10	0.49
	Box-Cox	-1.66	0.72	-1.78	0.42	-2.97	0.75
	ZL	0.08	1.42	0.36	0.68	0.73	0.83
	LZL	0.15	3.84	0.10	2.46	0.94	3.03
	ECDF	0.06	3.68	0.02	2.40	0.96	2.99
	MNLE	0.15	3.68	0.04	2.38	0.96	2.99
	Kernel	-1.24	1.88	-1.07	1.13	-0.89	1.56
	MSLE	-1.24	1.88	-1.07	1.14	-0.90	1.56
Beta (0.7)	BP	0.46	0.44	0.44	0.24	0.62	0.34
	Box-Cox	-1.65	0.53	-1.77	0.36	-2.02	0.55
	ZL	-0.24	0.91	0.06	0.45	0.34	0.63
	LZL	-0.20	2.12	0.01	1.32	0.80	1.50
	ECDF	-0.46	1.93	-0.12	1.26	0.68	1.47
	MNLE	-0.39	1.93	-0.09	1.25	0.69	1.47
	Kernel	-1.16	0.99	-0.82	0.60	-0.78	0.84
	MSLE	-1.17	1.00	-0.82	0.60	-0.78	0.84

S2 Proof of Proposition 1 in the main article

For (a). The proof is straightforward and we omit the details.

For (b). Let $l_2(\alpha_0, \dots, \alpha_N) = \log L_2(\alpha_0, \dots, \alpha_N)$. Since there is no constraint on α_0 , and $l_2(\alpha_0, \dots, \alpha_N)$ is a concave function of $(\alpha_0, \dots, \alpha_N)$, $\hat{\alpha}_0$ has to satisfy the first-order condition. That is

$$\frac{\partial l_2(\hat{\alpha}_0, \hat{\alpha}_1, \dots, \hat{\alpha}_N)}{\partial \alpha_0} = 0. \quad (\text{S1})$$

Note that

$$\frac{\partial}{\partial \alpha_0} l_2(\alpha_0, \alpha_1, \dots, \alpha_N) = \sum_{i=1}^m b_i - \sum_{i=1}^m (a_i + b_i) \theta(t_i).$$

Therefore, (S1) leads to

$$0 = \sum_{i=1}^m b_i - \sum_{i=1}^m (a_i + b_i) \hat{\theta}(t_i),$$

which, together with the facts that $\sum_{i=1}^m b_i = n_1$ and $\lambda = n_1/n$, imply that $\sum_{i=1}^m \hat{\phi}_i \hat{\theta}(t_i) = \lambda$. This finishes the proof.

S3 Proof of Theorem 1 in the main article

We first define some notation. We denote

$$d^2(\hat{\theta}, \theta_0) = \int_0^1 \left\{ \hat{\theta}(x) - \theta_0(x) \right\}^2 dG(x).$$

Let $R(x) = \log\{f_1(x)/f_0(x)\}$,

$$\theta_N(x) = \frac{\lambda \exp \left\{ \sum_{l=0}^N R(l/N) B_l(x; N) \right\}}{1 - \lambda + \lambda \exp \left\{ \sum_{l=0}^N R(l/N) B_l(x; N) \right\}}, \quad (\text{S2})$$

and

$$\mathcal{B}_N = \left\{ \theta(x) = \frac{\lambda \exp \left\{ \sum_{l=0}^N \beta_l B_l(x; N) \right\}}{1 - \lambda + \lambda \exp \left\{ \sum_{l=0}^N \beta_l B_l(x; N) \right\}} : \beta_0 \leq \beta_1 \cdots \leq \beta_N \right\}.$$

By Condition A3, $\theta_N(x) \in \mathcal{B}_N$. Further let

$$\ell_n(\theta) = \frac{1}{n} \sum_{i=1}^m \log[\{\theta(t_i)\}^{b_i} \{1 - \theta(t_i)\}^{a_i}].$$

Then

$$\hat{\theta}(x) = \arg \max_{\theta(x) \in \mathcal{B}_N} \ell_n(\theta).$$

By Condition A1, $n_1/n \rightarrow \lambda \in (0, 1)$ as $n \rightarrow \infty$. As we discussed in Section 2.1 of the main paper, we write $\lambda = n_1/n$ and assume that it is constant, since it does not affect our technical development. Define

$$\gamma_0(x; \theta) = 4(1 - \lambda) \left\{ \sqrt{\frac{1 - \theta(x)}{1 - \theta_0(x)}} - 1 \right\}$$

and

$$\gamma_1(x; \theta) = 4\lambda \left\{ \sqrt{\frac{\theta(x)}{\theta_0(x)}} - 1 \right\}.$$

The proof of Theorem 1 consists of three steps.

Step 1. We argue that

$$d^2(\hat{\theta}, \theta_0) \leq \int \gamma_0(x; \hat{\theta}) d\{\tilde{F}_0(x) - F_0(x)\} + \int \gamma_1(x; \hat{\theta}) d\{\tilde{F}_1(x) - F_1(x)\} + 2\{\ell_n(\theta_0) - \ell_n(\theta_N)\},$$

where $\tilde{F}_0(x)$ and $\tilde{F}_1(x)$ are the empirical cumulative distribution functions of $\{X_1, \dots, X_{n_0}\}$ and $\{Y_1, \dots, Y_{n_1}\}$, respectively.

Step 2. We use results from empirical processes to show that

$$\int \gamma_0(x; \hat{\theta}) d\{\tilde{F}_0(x) - dF_0(x)\} = o_p(1) \quad (\text{S3})$$

and

$$\int \gamma_1(x; \hat{\theta}) d\{\tilde{F}_1(x) - dF_1(x)\} = o_p(1). \quad (\text{S4})$$

Step 3. We further show that

$$\ell_n(\theta_0) - \ell_n(\theta_N) = o_p(1). \quad (\text{S5})$$

We start with Step 1. Since $\hat{\theta}(x)$ maximizes $\ell_n(\theta)$ over \mathcal{B}_N and $\theta_N(x) \in \mathcal{B}_N$, we have

$$\begin{aligned} \ell_n(\theta_0) - \ell_n(\theta_N) &\geq \ell_n(\theta_0) - \ell_n(\hat{\theta}) \\ &= -\frac{1}{n} \sum_{i=1}^m \left\{ b_i \log \frac{\hat{\theta}(t_i)}{\theta_0(t_i)} + a_i \log \frac{1 - \hat{\theta}(t_i)}{1 - \theta_0(t_i)} \right\} \\ &= -\frac{1}{n} \left\{ \sum_{i=1}^{n_1} \log \frac{\hat{\theta}(Y_i)}{\theta_0(Y_i)} + \sum_{j=1}^{n_0} \log \frac{1 - \hat{\theta}(X_j)}{1 - \theta_0(X_j)} \right\} \\ &= -\left\{ \lambda \int \log \frac{\hat{\theta}(x)}{\theta_0(x)} d\tilde{F}_1(x) + (1 - \lambda) \int \log \frac{1 - \hat{\theta}(x)}{1 - \theta_0(x)} d\tilde{F}_0(x) \right\}. \end{aligned}$$

Applying the inequality $0.5 \log x \leq \sqrt{x} - 1$ for $x > 0$, we further get

$$\begin{aligned} 2\{\ell_n(\theta_0) - \ell_n(\theta_N)\} &\geq -\int \gamma_1(x; \hat{\theta}) d\tilde{F}_1(x) - \int \gamma_0(x; \hat{\theta}) d\tilde{F}_0(x) \\ &= -\int \gamma_1(x; \hat{\theta}) d\{\tilde{F}_1(x) - dF_1(x)\} - \int \gamma_1(x; \hat{\theta}) dF_1(x) \\ &\quad - \int \gamma_0(x; \hat{\theta}) d\{\tilde{F}_0(x) - F_0(x)\} - \int \gamma_0(x; \hat{\theta}) dF_0(x), \end{aligned}$$

which leads to

$$\begin{aligned} -\int \gamma_0(x; \hat{\theta}) dF_0(x) - \int \gamma_1(x; \hat{\theta}) dF_1(x) &\leq \int \gamma_1(x; \hat{\theta}) d\{\tilde{F}_1(x) - dF_1(x)\} \\ &\quad + \int \gamma_0(x; \hat{\theta}) d\{\tilde{F}_0(x) - F_0(x)\} \\ &\quad + 2\{\ell_n(\theta_0) - \ell_n(\theta_N)\}. \end{aligned}$$

To finish the proof of Step 1, it suffices to show that

$$d^2(\hat{\theta}, \theta_0) \leq -\int \gamma_0(x; \hat{\theta}) dF_0(x) - \int \gamma_1(x; \hat{\theta}) dF_1(x). \quad (\text{S6})$$

By the definition of $\theta_0(x)$, we have that

$$dF_1(x) = \frac{\theta_0(x)/\{1 - \theta_0(x)\}}{\lambda/(1 - \lambda)} dF_0(x) \quad (\text{S7})$$

and

$$dG(x) = \lambda dF_1(x) + (1 - \lambda)dF_0(x) = \frac{1 - \lambda}{1 - \theta_0(x)} dF_0(x). \quad (\text{S8})$$

Note that (S7) and (S8) imply

$$\begin{aligned} - \int \gamma_1(x; \hat{\theta}) dF_1(x) &= \int 4\lambda \frac{\theta_0(x)/\{1 - \theta_0(x)\}}{\lambda/(1 - \lambda)} \left\{ 1 - \sqrt{\frac{\hat{\theta}(x)}{\theta_0(x)}} \right\} dF_0(x) \\ &= 4 \int \theta_0(x) \left\{ 1 - \sqrt{\frac{\hat{\theta}(x)}{\theta_0(x)}} \right\} dG(x) \end{aligned}$$

and

$$- \int \gamma_0(x; \hat{\theta}) dF_0(x) = 4 \int \{1 - \theta_0(x)\} \left\{ 1 - \sqrt{\frac{1 - \hat{\theta}(x)}{1 - \theta_0(x)}} \right\} dG(x).$$

Hence,

$$\begin{aligned} & - \int \gamma_0(x; \hat{\theta}) dF_0(x) - \int \gamma_1(x; \hat{\theta}) dF_1(x) \\ &= 4 \int \left[1 - \sqrt{\hat{\theta}(x)\theta_0(x)} - \sqrt{\{1 - \hat{\theta}(x)\}\{1 - \theta_0(x)\}} \right] dG(x) \\ &= 2 \int \left\{ \sqrt{\hat{\theta}(x)} - \sqrt{\theta_0(x)} \right\}^2 dG(x) + 2 \int \left\{ \sqrt{1 - \hat{\theta}(x)} - \sqrt{1 - \theta_0(x)} \right\}^2 dG(x). \end{aligned}$$

Using the facts that both $\theta_0(x)$ and $\hat{\theta}(x) \in [0, 1]$, we get that

$$\begin{aligned} & - \int \gamma_0(x; \hat{\theta}) dF_0(x) - \int \gamma_1(x; \hat{\theta}) dF_1(x) \\ & \geq 2 \int \frac{1}{4} \left\{ \hat{\theta}(x) - \theta_0(x) \right\}^2 dG(x) + 2 \int \frac{1}{4} \left\{ \hat{\theta}(x) - \theta_0(x) \right\}^2 dG(x) \\ & = d^2(\hat{\theta}, \theta_0). \end{aligned}$$

This finishes the proof of (S6), and hence that of Step 1.

We now move to Step 2. Let

$$\mathcal{H} = \{h(x) : h(x) \text{ is non-decreasing on } [0, 1] \text{ and } h(x) \in [0, 1]\}.$$

Using Theorems 2.2 and 9.24 of Kosorok (2008), we have that the class \mathcal{H} is P -Glivenko–Cantelli (P -G-C) for $P = F_0$ and F_1 . That is,

$$\sup_{h(x) \in \mathcal{H}} \left| \int h(x) d\{\tilde{F}_0(x) - F_0(x)\} \right| = o_p(1) \quad \text{and} \quad \sup_{h(x) \in \mathcal{H}} \left| \int h(x) d\{\tilde{F}_1(x) - F_1(x)\} \right| = o_p(1).$$

Since $\mathcal{B}_N \subset \mathcal{H}$, the class \mathcal{B}_N is also P -G-C for $P = F_0$ and F_1 .

Let

$$\Gamma_0 = \{\gamma_0(x; \theta) : \theta(x) \in \mathcal{B}_N\}.$$

We notice that $|\gamma_0(x; \theta)| \leq 4(1 - \lambda)[1/\{1 - \theta_0(x)\} + 1]$ and

$$\begin{aligned} \int 4(1 - \lambda)[1/\{1 - \theta_0(x)\} + 1] dF_0(x) &= 4(1 - \lambda) + \int 4(1 - \lambda)/\{1 - \theta_0(x)\} dF_0(x) \\ &= 4(1 - \lambda) + \int 4 dG(x) \\ &= 4 + 4(1 - \lambda) < \infty. \end{aligned}$$

That is, the class Γ_0 has an integrable envelope. Applying Corollary 9.27 of Kosorok (2008), we then get that Γ_0 is F_0 -G-C, i.e.,

$$\sup_{\theta(x) \in \Gamma_0} \left| \int \gamma_0(x; \theta) d\{\tilde{F}_0(x) - F_0(x)\} \right| = o_p(1),$$

which implies that

$$\int \gamma_0(x; \hat{\theta}) d\{\tilde{F}_0(x) - F_0(x)\} = o_p(1).$$

Similarly,

$$\int \gamma_1(x; \hat{\theta}) d\{\tilde{F}_1(x) - F_1(x)\} = o_p(1).$$

This finishes Step 2.

We consider Step 3. It can be checked that

$$\begin{aligned} \ell_n(\theta_0) - \ell_n(\theta_N) &= -\frac{\lambda}{n_1} \sum_{i=1}^{n_1} \log \frac{\theta_N(Y_i)}{\theta_0(Y_i)} - \frac{1-\lambda}{n_0} \sum_{j=1}^{n_0} \log \frac{1-\theta_N(X_j)}{1-\theta_0(X_j)} \\ &= -\lambda \int \log \frac{\theta_N(x)}{\theta_0(x)} d\tilde{F}_1(x) - (1-\lambda) \int \log \frac{1-\theta_N(x)}{1-\theta_0(x)} d\tilde{F}_0(x). \end{aligned}$$

By Condition A3 and the construction of $\theta_N(x)$ in (S2), we have

$$\theta_0(x) \in [\delta, 1-\delta] \quad \text{and} \quad \theta_N(x) \in [\delta, 1-\delta],$$

where $\delta > 0$ is provided in Condition A3.

Let

$$\mathcal{H}^* = \{h(x) : h(x) \text{ is non-decreasing on } [0,1] \text{ and } h(x) \in [\delta, 1-\delta]\}.$$

Then $\mathcal{H}^* \subset \mathcal{H}$. Hence, the class \mathcal{H}^* is P -G-C for $P = F_0$ and F_1 . Note that for any $h(x) \in \mathcal{H}^*$, both $|\log\{h(x)/\theta_0(x)\}|$ and $|\log\{[1-h(x)]/[1-\theta_0(x)]\}|$ are bounded functions. Using Corollary 9.27 of Kosorok (2008), we further have the two classes

$$\left\{ \log \frac{h(x)}{\theta_0(x)} : h(x) \in \mathcal{H}^* \right\} \quad \text{and} \quad \left\{ \log \frac{1-h(x)}{1-\theta_0(x)} : h(x) \in \mathcal{H}^* \right\}$$

are also P -G-C for $P = F_0$ and F_1 , which implies that

$$\int \log \frac{\theta_N(x)}{\theta_0(x)} d\{\tilde{F}_1(x) - F_1(x)\} = o_p(1) \quad \text{and} \quad \int \log \frac{1-\theta_N(x)}{1-\theta_0(x)} d\{\tilde{F}_0(x) - F_0(x)\} = o_p(1).$$

Hence,

$$\begin{aligned} \ell_n(\theta_0) - \ell_n(\theta_N) &= -\lambda \int \log \frac{\theta_N(x)}{\theta_0(x)} dF_1(x) - (1-\lambda) \int \log \frac{1-\theta_N(x)}{1-\theta_0(x)} dF_0(x) + o_p(1) \\ &= -\int \left[\theta_0(x) \log \frac{\theta_N(x)}{\theta_0(x)} + \{1-\theta_0(x)\} \log \frac{1-\theta_N(x)}{1-\theta_0(x)} \right] dG(x) + o_p(1). \end{aligned}$$

To finish Step 3, it is sufficient to show that

$$\int \left[\theta_0(x) \log \frac{\theta_N(x)}{\theta_0(x)} + \{1-\theta_0(x)\} \log \frac{1-\theta_N(x)}{1-\theta_0(x)} \right] dG(x) = o(1).$$

Recall that $R(x) = \log\{f_1(x)/f_0(x)\}$. Let

$$R_N(x) = \sum_{l=0}^N R(l/N) B_l(x; N).$$

According to Lorentz (1986), under Condition A3, we have

$$\lim_{N \rightarrow \infty} \sup_{x \in [0,1]} |R(x) - R_N(x)| = 0. \quad (\text{S9})$$

Further let

$$g(t) = \frac{\lambda \exp(t)}{1 - \lambda + \lambda \exp(t)}.$$

Then, $\theta_0(x) = g(R(x))$ and $\theta_N(x) = g(R_N(x))$. It can be easily verified that $|g'(t)| \leq 1$ for all t , which, together with (S9), implies that

$$\lim_{N \rightarrow \infty} \sup_{x \in [0,1]} |\theta_N(x) - \theta_0(x)| = 0. \quad (\text{S10})$$

Using the second-order Taylor expansion, we get

$$\begin{aligned} & \left| \int \left[\theta_0(x) \log \frac{\theta_N(x)}{\theta_0(x)} + \{1 - \theta_0(x)\} \log \frac{1 - \theta_N(x)}{1 - \theta_0(x)} \right] dG(x) \right| \\ &= 0.5 \int \left[\frac{\theta_0(x)}{\xi_N^2(x)} + \frac{1 - \theta_0(x)}{\{1 - \xi_N(x)\}^2} \right] \{\theta_N(x) - \theta_0(x)\}^2 dG(x) \\ &\leq \frac{0.5}{\delta^2} \int \{\theta_N(x) - \theta_0(x)\}^2 dG(x) \end{aligned} \quad (\text{S11})$$

where $\xi_N(x)$ is a function between $\theta_0(x)$ and $\theta_N(x)$, and we have used Condition A3 in the last step. Combining (S10) and (S11) leads to

$$\left| \int \left[\theta_0(x) \log \frac{\theta_N(x)}{\theta_0(x)} + \{1 - \theta_0(x)\} \log \frac{1 - \theta_N(x)}{1 - \theta_0(x)} \right] dG(x) \right| \leq \frac{0.5}{\delta^2} \left\{ \sup_{x \in [0,1]} |\theta_N(x) - \theta_0(x)| \right\}^2 \rightarrow 0$$

as $N \rightarrow \infty$. This finishes the proof of Step 3, and hence the proof of Theorem 1.

S4 Proof of Theorem 2 in the main article

Part (a) We concentrate on the consistency of $\hat{F}_1(x)$; the consistency of $\hat{F}_0(x)$ follows similarly.

Let

$$\tilde{G}(x) = \lambda \tilde{F}_1(x) + (1 - \lambda) \tilde{F}_0(x) = \sum_{i=1}^m \frac{a_i + b_i}{n} I(t_i \leq x).$$

Note that for any u ,

$$\begin{aligned} \hat{F}_1(u) &= \sum_{i=1}^m \hat{p}_{i1} I(t_i \leq u) \\ &= \sum_{i=1}^m \frac{1}{\lambda} \frac{a_i + b_i}{n} \hat{\theta}(t_i) I(t_i \leq u) \\ &= \int \frac{1}{\lambda} \hat{\theta}(x) I(x \leq u) d\tilde{G}(x). \end{aligned}$$

Recall

$$F_1(u) = \int \frac{1}{\lambda} \theta_0(x) I(x \leq u) dG(x).$$

Then

$$\hat{F}_1(u) - F_1(u) = \frac{1}{\lambda} \int \{\hat{\theta}(x) - \theta_0(x)\} I(x \leq u) dG(x) \quad (\text{S12})$$

$$+ \frac{1}{\lambda} \int \hat{\theta}(x) I(x \leq u) d\{\tilde{G}(x) - G(x)\}. \quad (\text{S13})$$

In the following, we show that the two terms in (S12) and (S13) are $o_p(1)$.

We first consider (S12). Note that

$$\begin{aligned} \left| \frac{1}{\lambda} \int \{\hat{\theta}(x) - \theta_0(x)\} I(x \leq u) dG(x) \right| &\leq \frac{1}{\lambda} \int |\hat{\theta}(x) - \theta_0(x)| I(x \leq u) dG(x) \\ &\leq \frac{1}{\lambda} \int |\hat{\theta}(x) - \theta_0(x)| dG(x) \\ &\leq \frac{1}{\lambda} \left[\int \{\hat{\theta}(x) - \theta_0(x)\}^2 dG(x) \right]^{1/2} \\ &= \lambda^{-1} d(\hat{\theta}, \theta_0) = o_p(1), \end{aligned} \quad (\text{S14})$$

where we have used the result in Theorem 1.

Next, we consider (S13). According to Lemmas 9.8 and 9.12 of Kosorok (2008),

$$\{I(x \leq u) : u \in \mathcal{R}\}$$

is a Vapnik–Chervonenkis subgraph class with the bounded envelope 1. By Theorems 8.14 and 9.2 of Kosorok (2008), we have that $\{I(x \leq u) : u \in \mathcal{R}\}$ is P -G-C for both F_0 and F_1 . Recall that in the proof of Theorem 1, we have argued that \mathcal{B}_N is also P -G-C for both F_0 and F_1 . Then by Corollary 9.27 of Kosorok (2008), $\{I(x \leq u)\theta(x) : \theta \in \mathcal{B}_N, u \in \mathcal{R}\}$ is P -G-C for both F_0 and F_1 . That is,

$$\sup_{\theta(x) \in \mathcal{B}_N, u \in \mathcal{R}} \left| \int I(x \leq u)\theta(x) d\{\tilde{F}_0(x) - F_0(x)\} \right| = o_p(1) \quad (\text{S15})$$

and

$$\sup_{\theta(x) \in \mathcal{B}_N, u \in \mathcal{R}} \left| \int I(x \leq u)\theta(x) d\{\tilde{F}_1(x) - F_1(x)\} \right| = o_p(1). \quad (\text{S16})$$

Note that (S15) and (S16) together lead to

$$\sup_{\theta(x) \in \mathcal{B}_N, u \in \mathcal{R}} \left| \int I(x \leq u)\theta(x) d\{\tilde{G}(x) - G(x)\} \right| = o_p(1),$$

which implies that

$$\sup_{u \in [0,1]} \left| \int I(x \leq u)\hat{\theta}(x) d\{\tilde{G}(x) - G(x)\} \right| = o_p(1). \quad (\text{S17})$$

Combining the results in (S12)–(S14) and (S17), we have

$$\sup_{x \in [0,1]} |\hat{F}_1(x) - F_1(x)| = o_p(1).$$

This completes the proof of Part (a).

Part (b) The proof for this part is very similar to the proof of Theorem 1 in Jokiel-Rokita and Pulit (2013). We omit the details here.

Part (c) Note that

$$\begin{aligned}
|\widehat{AUC} - AUC| &= \left| \int_0^1 \widehat{ROC}(s) - ROC(s) ds \right| \\
&\leq \int_0^1 |\widehat{ROC}(s) - ROC(s)| ds \\
&\leq \int_0^1 \sup_{s \in [0,1]} |\widehat{ROC}(s) - ROC(s)| ds \\
&\leq \sup_{s \in [0,1]} |\widehat{ROC}(s) - ROC(s)| \\
&= o_p(1).
\end{aligned}$$

Part (d) Let $A_n = \left\{ \inf_{x \in [0,1]} \hat{\theta}(x) < \lambda < \sup_{x \in [0,1]} \hat{\theta}(x) \right\}$. We first show that

$$\lim_{n \rightarrow \infty} P(A_n) = 1, \quad (\text{S18})$$

which implies that the probability that the solution of $\hat{\theta}(x) = \lambda$ exists in $[0, 1]$ approaches to 1 as n goes to infinity. Define

$$A_{n1} = \left\{ \inf_{x \in [0,1]} \hat{\theta}(x) \geq \lambda \right\}$$

and

$$A_{n2} = \left\{ \sup_{x \in [0,1]} \hat{\theta}(x) \leq \lambda \right\}.$$

It suffices to show that

$$\lim_{n \rightarrow \infty} P(A_{n1}) = 0, \quad (\text{S19})$$

and

$$\lim_{n \rightarrow \infty} P(A_{n2}) = 0. \quad (\text{S20})$$

We concentrate on (S19); the proof for (S20) follows similarly.

By Condition A4, there exists $\epsilon_0 > 0$ such that $\theta_0(x)$ is strictly increasing on $[C - \epsilon_0, C + \epsilon_0]$. Hence, $\theta_0(C) - \theta_0(C - \epsilon_0) > 0$. By the continuity and monotonicity of $\theta_0(x)$, there exists $0 < \delta_0 < \epsilon_0$ such that

$$0 < \theta_0(x) - \theta_0(C - \epsilon_0) \leq \frac{\theta_0(C) - \theta_0(C - \epsilon_0)}{2}$$

for any $x \in [C - \epsilon_0, C - \epsilon_0 + \delta_0]$, which together with the fact $\theta_0(C) = \lambda$ imply that

$$\lambda - \theta_0(x) = \theta_0(C) - \theta_0(x) \geq \frac{\theta_0(C) - \theta_0(C - \epsilon_0)}{2}, \quad \forall x \in [C - \epsilon_0, C - \epsilon_0 + \delta_0]. \quad (\text{S21})$$

Let $\delta_1 = 0.25\delta_0 \{\theta_0(C) - \theta_0(C - \epsilon_0)\}^2 > 0$. Then (S21) implies that

$$\begin{aligned}
P(A_{n1}) &\leq P \left(\int_{C-\epsilon_0}^{C-\epsilon_0+\delta_0} \left\{ \hat{\theta}(x) - \theta_0(x) \right\}^2 dx \geq \delta_1 \right) \\
&\leq P \left(\int_0^1 \left\{ \hat{\theta}(x) - \theta_0(x) \right\}^2 dx \geq \delta_1 \right) \\
&= P \left(d^2(\hat{\theta}, \theta_0) \geq \delta_1 \right).
\end{aligned}$$

By Theorem 1, we get

$$\lim_{n \rightarrow \infty} P(A_{n1}) = 0.$$

This finishes the proof of (S19) and hence that of (S18). With the result in (S18), without loss of generality, we assume that the solution to $\hat{\theta}(x) = \lambda$ exists, i.e.,

$$\hat{\theta}(\hat{C}) = \lambda.$$

We now move to the consistency of \hat{C} . Equivalently, we need to show that for any $\epsilon > 0$,

$$\lim_{n \rightarrow \infty} P(\hat{C} \geq C + \epsilon) = 0, \quad (\text{S22})$$

and

$$\lim_{n \rightarrow \infty} P(\hat{C} \leq C - \epsilon) = 0. \quad (\text{S23})$$

We first consider (S22). Note that

$$\begin{aligned} P(\hat{C} \geq C + \epsilon) &\leq P(\hat{\theta}(\hat{C}) \geq \hat{\theta}(C + \epsilon)) \\ &= P(\hat{\theta}(C + \epsilon) - \lambda \leq 0) \\ &\leq P\left(\int_C^{C+\epsilon} \{\theta_0(x) - \hat{\theta}(x)\}^2 dx \geq \int_C^{C+\epsilon} \{\theta_0(x) - \lambda\}^2 dx\right) \\ &\leq P\left(\int_0^1 \{\theta_0(x) - \hat{\theta}(x)\}^2 dx \geq \int_C^{C+\epsilon} \{\theta_0(x) - \lambda\}^2 dx\right) \\ &= P\left(d^2(\hat{\theta}, \theta_0) \geq \int_C^{C+\epsilon} \{\theta_0(x) - \lambda\}^2 dx\right). \end{aligned}$$

Condition A4 implies that $\int_C^{C+\epsilon} \{\theta_0(x) - \lambda\}^2 dx > 0$. By Theorem 1, we have

$$\lim_{n \rightarrow \infty} P(\hat{C} \geq C + \epsilon) = 0.$$

This completes (S22). The proof of (S23) follows similarly.

Finally, we consider the consistency of \hat{J} . Note that

$$\begin{aligned} \hat{J} - J &= \{\hat{F}_0(\hat{C}) - \hat{F}_1(\hat{C})\} - \{F_0(C) - F_1(C)\} \\ &= \{\hat{F}_0(\hat{C}) - \hat{F}_1(\hat{C})\} - \{F_0(\hat{C}) - F_1(\hat{C})\} \\ &\quad + \{F_0(\hat{C}) - F_1(\hat{C})\} - \{F_0(C) - F_1(C)\}. \end{aligned}$$

Then

$$|\hat{J} - J| \leq |F_0(\hat{C}) - F_0(C)| + |F_1(\hat{C}) - F_1(C)| \quad (\text{S24})$$

$$+ \sup_{x \in [0,1]} |\hat{F}_0(x) - F_0(x)| + \sup_{x \in [0,1]} |\hat{F}_1(x) - F_1(x)|. \quad (\text{S25})$$

By the consistency of \hat{C} and the continuous mapping theorem, the term in (S24) is $o_p(1)$. The term in (S25) is also $o_p(1)$ by the results in Part (a). Hence $\hat{J} - J = o_p(1)$ as claimed.

References

- Jokiel-Rokita, A. and M. Pulit (2013). Nonparametric estimation of the roc curve based on smoothed empirical distribution functions. *Statistics and Computing* 23, 703–712.
- Kosorok, M. R. (2008). *Introduction to Empirical Processes and Semiparametric Inference*. New York: Springer.
- Lin, H., X.-H. Zhou, and G. Li (2012). A direct semiparametric receiver operating characteristic curve regression with unknown link and baseline functions. *Statistica Sinica* 22, 1427–1456.
- Lorentz, G. G. (1986). *Bernstein Polynomials* (Second ed.). New York: Chelsea Publishing Company.